


## Article

# Enhanced Exhaust after-Treatment Warmup in a Heavy-Duty Diesel Engine System via Miller Cycle and Delayed Exhaust Valve Opening

Hasan Ustun Basaran 

Department of Naval Architecture and Marine Engineering, Faculty of Naval Architecture and Maritime, Izmir Katip Celebi University, Cigli, 35620 Izmir, Turkey; hustun.basaran@ikcu.edu.tr

**Abstract:** The exhaust after-treatment (EAT) threshold temperature is a significant concern for highway vehicles to meet the strict emission norms. Particularly at cold engine start and low loads, EAT needs to be improved above 250 °C to reduce the tailpipe emission rates. Conventional strategies such as electrical heating, exhaust throttling, or late fuel injection mostly need a high fuel penalty for fast EAT warmup. The objective of this work is to demonstrate using a numerical model that a combination of the Miller cycle and delayed exhaust valve opening (DEVO) can improve the tradeoff between EAT warmup and fuel consumption penalty. A relatively low-load working condition (1200 RPM speed and 2.5 bar *BMEP*) is maintained in the diesel engine model. The Miller cycle via retarded intake valve closure (RIVC) is noticeably effective in increasing exhaust temperature (as high as 55 °C). However, it also dramatically reduces the exhaust flow rate (over 30%) and, thus, is ineffective for rapid EAT warmup. DEVO has the potential to enhance EAT warmup via increased exhaust temperature and increased exhaust flow rate. However, it considerably decreases the brake thermal efficiency (BTE)—by up to 5%—due to high pumping loss in the system. The RIVC + DEVO combined technique can elevate the exhaust temperature above 250 °C with improved fuel consumption—up to 10%—compared to DEVO alone as it requires a relatively lower rise in pumping loss. The combined method is also superior to RIVC alone. Unlike RIVC alone, the RIVC + DEVO combined mode does not need the extreme use of RIVC to increase engine-out temperature above 250 °C and, thus, provides relatively higher heat transfer rates (up to 103%) to the EAT system through a higher exhaust flow rate. The RIVC + DEVO combined method can be technically more difficult to implement compared to other methods. However, it has the potential to maintain accelerated EAT warmup with improved BTE and, thus, can keep emission rates at low levels during cold start and low loads.

**Keywords:** heavy-duty diesel engines; exhaust temperature; exhaust flow rate; after-treatment thermal management; variable valve timing



**Citation:** Basaran, H.U. Enhanced Exhaust after-Treatment Warmup in a Heavy-Duty Diesel Engine System via Miller Cycle and Delayed Exhaust Valve Opening. *Energies* **2023**, *16*, 4542. <https://doi.org/10.3390/en16124542>

Academic Editors: Enhua Wang and Baofeng Yao

Received: 30 April 2023

Revised: 29 May 2023

Accepted: 31 May 2023

Published: 6 June 2023



**Copyright:** © 2023 by the author. Licensee MDPI, Basel, Switzerland. This article is an open access article distributed under the terms and conditions of the Creative Commons Attribution (CC BY) license (<https://creativecommons.org/licenses/by/4.0/>).

## 1. Introduction

At present, most modern automotive vehicles and marine vessels are driven by diesel engines due to reliable, fuel-saving, and economic operation. However, highly strict emission norms present a significant challenge for the widespread usage of diesel engines in both highway and maritime transport [1,2]. Considering the possible tighter future emission regulations, engine producers and researchers constantly seek new strategies to reduce emission rates in both light-duty and heavy-duty diesel engine systems [3,4].

The application of exhaust gas recirculation (EGR) is a common and an effective method to decrease emission rates in diesel engine systems [5]. Although EGR is highly useful to reduce nitrogen oxide (NO<sub>x</sub>) rates via reduced in-cylinder temperature, excessive use of it generally results in rise in particulate matter (PM) flow rates [6]. Another effective way to control engine-out emission rates is to utilize advanced and relatively new low-temperature combustion (LTC) techniques [7]. Replacing diesel completely with alternative

fuels, particularly with methane, methanol, and hydrogen, or using blended ratios is also a focus of engine researchers to improve the NO<sub>x</sub>, PM, hydrocarbon (HC), and carbon monoxide (CO) rates in automotive vehicles [8–10]. Although those strategies are helpful to limit harmful diesel tailpipe gas, they cannot always curb emission rates adequately at all engine speed and engine loading cases. Thus, diesel vehicles are generally equipped with a reliable emission-reducing component: an exhaust after-treatment (EAT) system [11]. Producers mostly depend on both aforementioned inner-engine methods and catalytic diesel after-treatment systems to meet the ever-tightening emission standards [12,13].

Exhaust units of diesel vehicles are normally outfitted with a three-way catalytic converter (TWC) system [14]. NO<sub>x</sub> is diminished through the catalytic reactions inside a selective catalytic reduction (SCR) unit on a TWC system. PM is reduced via trapping the soot on the filters of a diesel particulate filter (DPF) unit. The third unit, a diesel oxidation catalyst (DOC), is responsible for decreasing the unburned hydrocarbons (UHCs) and CO rates. Those aforementioned EAT units in general can successfully lower the emission rates. However, the catalysts inside those units are mostly activated after a certain temperature (~250 °C) [15,16]. Furthermore, effective emission conversion is generally maintained within a certain temperature range (250–450 °C) at those systems [17–19]. At high loads or high-speed operations, this is not problematic in diesel vehicles since exhaust temperatures and exhaust flow rates are already high; thus, high-temperature EAT performance can be sustained. However, particularly at cold start and low loads, exhaust gas flow through the EAT unit remains mostly at a low temperature (<250 °C) due to the poor fuel injection rate and elevated in-cylinder air-to-fuel ratio (AFR). As such, EAT operation is ineffective, and emission control is affected negatively. A rise in after-treatment inlet temperature and flow rate is required to maintain fast EAT warmup and, thus, effective emission control in diesel vehicles [20–22].

Delayed fuel injection (DFI) is one of the proven methods to increase exhaust temperature in diesel engines [23]. However, temperature rise is mostly slight or moderate in this method, and a high fuel penalty is required to keep constant system performance due to degraded combustion [24]. In particular, late post fuel injection was recently examined, and promising experimental results on exhaust temperature rise were obtained at low loads [25–27]. Some external measures—namely, electrical heating, afterburner, and heating storage units—can also be preferred in automotive vehicles to warm up exhaust components [28–31]. However, those systems mostly need additional energy consumption and extra elements to be placed on diesel exhaust units, which is cost-ineffective. Those systems may also require certain design characteristics due to the space needed for operation close to the exhaust units in vehicles [32].

One recent engine-dependent method to elevate diesel exhaust temperature is variable valve timing (VVT) [33]. It can be seen that VVT is effective in changing flow rates at ports and in-cylinder combustion. Therefore, it is practical to modulate engine-out temperature. Early exhaust valve opening (EEVO) is a typical and common VVT-based strategy to enhance exhaust temperature [34]. It is possible to elevate EAT inlet temperature up to 65 °C at low loads through use of EEVO, yet with a considerable reduction (up to 5%) in thermal efficiency due to reduced expansion work [35]. Unlike EEVO, the Miller cycle via early intake valve closure (EIVC) improves thermal efficiency, while turbine-out temperature is maintained above 250 °C at low loads [36]. The fuel-saving performance of EIVC is attributed to low pumping loss through decreased in-cylinder air charge. Similar to EIVC, cylinder deactivation (CDA)—a type of VVT—enables reduced airflow through completely disconnecting the charge flow in some of the cylinders [37]. It not only raises the exhaust temperature significantly, but also results in fuel efficiency particularly at low loads [38,39]. However, in most of those aforementioned techniques, there is usually a need for extreme delay or advance of valve timings—such as in EEVO and EIVC modes—or the need to control both valve timing and fuel injection—such as in CDA mode—for high exhaust temperature improvement. Moreover, the EAT warmup period is degraded in EIVC or CDA modes due to highly reduced exhaust flow rates [40]. Despite those negative

effects, VVT is a proven technique to increase engine-out temperature. Some types of VVT—such as retarded intake valve closure (RIVC), another form of Miller cycle—were experimentally shown to be fuel-saving, highlighting it as a reliable, cost-effective, and promising technology [41,42].

The application of multiple VVT for enhanced EAT warmup in low-load conditions is relatively inadequate in the literature [22,43]. Previous works demonstrated that the implementation of single-VVT has a definite potential on EAT warmup. However, single-valve modulations increase only the exhaust temperature without considering mass flow rate at the EAT inlet and, therefore, decelerate after-treatment warmup [44] or need a dramatic fuel consumption penalty for a moderate improvement in EAT warmup [45]. The implementation of combined VVT techniques can be a solution for fast EAT warmup without suffering an extreme fuel consumption penalty at low loads. It can be proposed that, instead of this difficult VVT combination, DFI can be applied more practically to increase  $T_{exhaust}$ . However, DFI can only obtain moderate exhaust temperature improvement and, thus, is mostly inadequate to improve  $T_{exhaust}$  above 250 °C. The fuel penalty due to DFI is generally high (above 10%), which is disadvantageous as a high fuel penalty increases both UHC and CO rates. DFI enhances exhaust temperatures through deteriorated in-cylinder combustion, which is prone to yield undesirable PM rates [46]. Thus, DFI alone is not generally seen as a viable strategy for  $T_{exhaust}$  improvement.

Considering the previous studies on exhaust thermal management, it can be seen that both the Miller cycle through RIVC and the delayed exhaust valve opening (DEVO) are proven methods to improve exhaust temperature at low loads [47,48]. RIVC is also an effective method to reduce NO<sub>x</sub> and soot rates [49]. DEVO has the benefit of lower soot compared to EEVO for high exhaust temperatures at low loads [50]. Thus, unlike EEVO, it can improve the tradeoff between NO<sub>x</sub> and PM rates until EAT is warmed up. However, it generally requires either an extreme delay of IVC in RIVC mode or an aggressive retardation of EVO in DEVO mode to achieve a significant temperature rise in exhaust units. Moreover, the exhaust flow rate plays a crucial role in EAT warmup. RIVC leads to dramatic airflow reduction and, thus, highly decreased exhaust flow rates. As such, RIVC alone is a good candidate for the EAT stay-warm period, but definitely not for the EAT get-warm period, which necessitates high exhaust flow rates [51]. DEVO increases both the exhaust temperature and the exhaust flow rate, which at first seems an attractive solution for improving the EAT get-warm period. However, overuse of DEVO causes a noticeable fuel penalty (over 20%), which is certainly cost-ineffective and not practical, while greatly increasing soot rates and requiring high EGR rates to control NO<sub>x</sub> rates until catalyst light-off is achieved [50].

This study aims to combine the two aforementioned VVT methods, namely, RIVC and DEVO, to enhance the tradeoff between EAT warmup and engine fuel consumption penalty. The combined RIVC + DEVO strategy requires excessive delay of neither IVC nor EVO to increase the exhaust temperature above 250 °C and maintain an adequately heated EAT unit. Additionally, fuel consumption is reduced compared to DEVO alone due to the improving effect of RIVC on engine pumping loss. For the same fuel consumption penalty, unlike the RIVC + DEVO method, neither DEVO/EEVO nor DFI can improve the exhaust temperature above 250 °C and sustain an overheated EAT unit. The RIVC + DEVO combined technique also better improves EAT warmup compared to the nominal, DEVO alone, or RIVC alone methods through increased heat transfer rates. The increased VVT complexity in the engine system is a serious disadvantage (its production and maintenance during operation are difficult). However, compared to outer-engine methods such as electrical heating or afterburners, it does not need an external fuel pump or an additional space in the system, which can be relatively advantageous for fuel economy and vehicle design. Therefore, the RIVC + DEVO combined method can be an alternative practical approach to enhance diesel EAT warmup at low-load operations of automotive and marine vehicles.

## 2. Methodology

### 2.1. Heavy-Duty Diesel Engine Model

A six-cylinder turbocharged compression–ignition (CI) engine was utilized for the proposed different VVT cases in the study. The main properties of the selected CI engine are stated in Table 1. The diesel engine was a heavy-duty (HD) type, commonly used in trucks, public buses, and small marine vessels during highway and marine transport. Table 1 explicitly shows the exact opening and closure timings of inlet and outlet valves in nominal mode. Only IVC and EVO were modulated in the study, whereas IVO and EVC were kept constant (valve opening/closing slopes are altered due to different IVC and EVO timings). The firing order of the cylinders (1-5-3-6-2-4) is also given in Table 1, where 1 denotes the upmost cylinder and 6 represents the downmost cylinder in the system.

**Table 1.** Diesel engine properties.

Model	Six-Cylinder CI Engine
Air intake	Turbocharged
Bore (mm)	107
Stroke (mm)	124
Connecting rod length (mm)	192
Compression ratio	17.3:1
Maximum engine speed (RPM)	2800
Maximum engine load (as <i>BMEP</i> ) (bar)	19.0
EVO	20 °CA BBDC
EVC	20 °CA ATDC
IVO	20 °CA BTDC
IVC	25 °CA ABDC
Start of injection (SOI)	3 °CA BTDC
Cylinder firing order	1-5-3-6-2-4

Previous studies on diesel exhaust temperature management mostly focused on engine operations at low loads [52,53]. Thus, similar to those works, a low-load operating case was selected for the analysis. The operation point for the engine at hand is given in Table 2. The engine *BMEP* per cylinder, namely, the potential of each cylinder to produce brake power, was maintained the same in all calculations, as 2.5 bar. During valve timing modulations, the fuel injection rate was increased or decreased as required to maintain engine load—*BMEP*—constant. It should be noted that automotive vehicles do not always work in steady states (as in this study); they usually need to go through a transient operation during inner-city traffic. For instance, delivery vehicles, urban buses, or shuttles are generally faced with stop-and-go cases, which can be better represented with transient operations. This work concentrates on the use of VVT in a steady low-load operation condition. However, VVT and CDA were examined in the literature and also found to be successful at transient operations [54,55]. Therefore, the application of VVT seems to be practical not only for constant-load cases, but also for variable-load cases.

**Table 2.** Steady-state working condition for the diesel engine.

Engine Speed (RPM)	Engine <i>BMEP</i> (Bar)
1200	2.5

Figure 1 illustrates the built-in engine model used in the study to examine the engine characteristics at turbine exit. The Lotus Engine Simulation (LES) program was used to carry out the whole analysis [56,57]. The flow through the intake and exhaust was achieved via 1D analysis in the program. Similar to a real engine case, intake fresh air was charged into the cylinders through separate intake pipes, and engine-out exhaust was discharged from the cylinders through separate exhaust pipes. Every cylinder featured two individual

intake and exhaust ports. Valves were placed between ports and cylinders. Six pairs of intake and exhaust valves were operated simultaneously—whether in nominal mode or in any VVT-based mode—in the system. Fuel injection timing was adjusted at 3 °CA BTDC and remained fixed in all calculations. LES enables a rapid engine model generation and has the advantage of producing and analyzing model results in a fast and detailed manner through its well-designed interface functionality [58]. This fast model building and running allows the user to relatively easily examine the impact of change of different parameters such as fuel injection timing, valve timing, or throttling valve opening percentage. LES is particularly beneficial to examine the effect of VVT on a diesel or a gasoline engine since it enables not only valve timing control, but also maximum valve lift and valve lift profile modulation, which are critical to prevent a possible piston-valve crash during VVT application and, thus, can better represent a real engine operation. Therefore, it has been utilized for the improvement of internal combustion engines by several researchers [59–61].

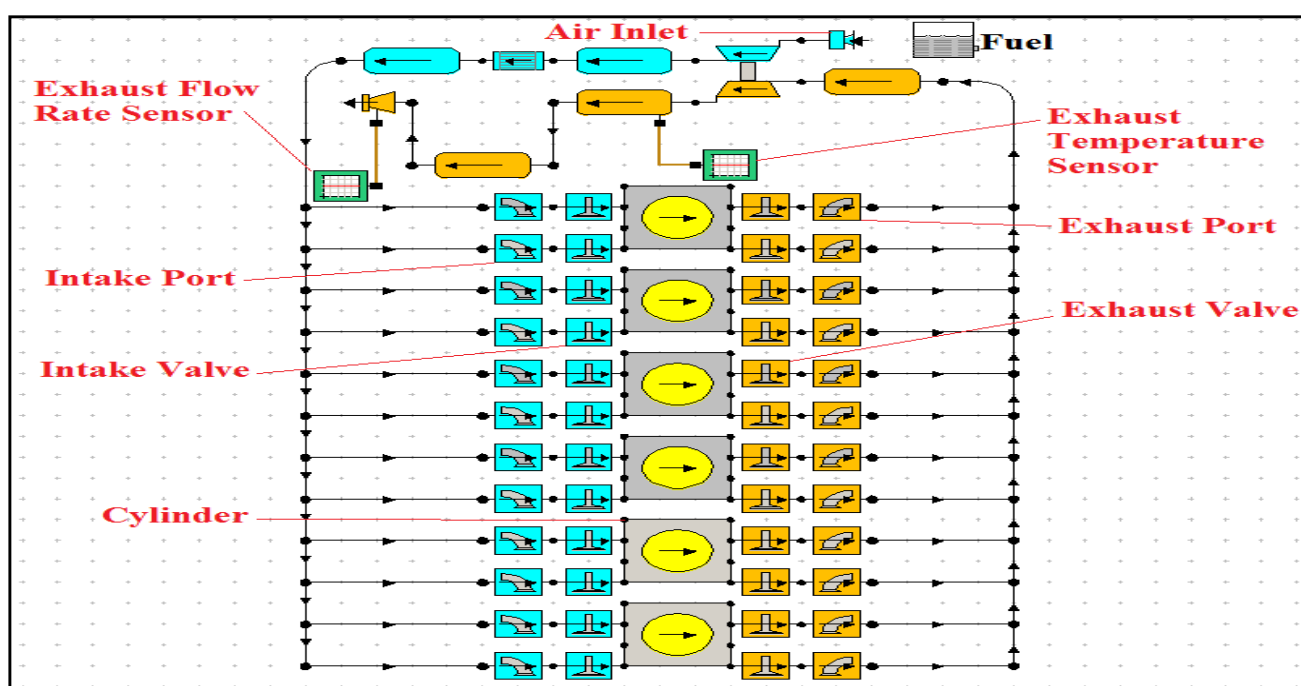


Figure 1. Built-in model of the engine.

HD diesel engine systems generally necessitate TWC units to reduce harmful pollutants of NO<sub>x</sub>, PM, CO, and UHCs. However, a TWC system (most common EAT unit in automotive vehicles) was not included to the model at hand. The primary focus of the simulation in Figure 1 is on temperature and flow rate of the exhaust gas at the turbine exit, which play a significant role on TWC warm up. Previous studies proved that those two parameters directly affect both the efficiency and the warmup characteristics of after-treatment systems [62]. Therefore, they should be primarily examined in order to achieve desired emission rates at low loads.

Two important sensors are placed in Figure 1 to evaluate the temperature and flow rate at the turbine outlet. The sensor on the right of the plot examines the variation of temperature at the turbocharger exit. At the outlet of the turbine, exhaust temperature and, thus, exhaust heat decrease due to the expansion process through the turbine. While it is essential to increase turbine power to supply more fresh air into the cylinders, it is equally essential to control the exhaust heat loss through the turbine in order to direct more heat to the EAT unit in a diesel engine system.

The sensor on the left of the plot is responsible for observing the change in exhaust flow rate at the EAT inlet. The system in Figure 1 does not include an external EGR system. Therefore, the mass flow rate at turbine exit is equal to that at the inlet of the EAT unit,

where the exhaust flow rate sensor is placed. It is noted that elevated exhaust energy and thus, elevated exhaust flow rate are needed at that point to accelerate the EAT warmup duration. Therefore, the change in exhaust rate is as essential as the change in engine-out temperature and should be considered for overall assessment of the EAT thermal management at different VVT modes.

## 2.2. Assumptions and Equations Utilized in the Model

Operating the engine in different VVT modes may result in slight or, for some cases, extreme changes in engine performance characteristics. Engine brake power,  $P_e$ , is one of those significant characteristics; it was calculated in the simulation as follows [63]:

$$P_e = (BMEPV_dNZ/n, 60), \quad (1)$$

where  $N$  is the engine speed, taken as constant and 1200 RPM during all calculations.  $BMEP$  denotes the engine loading, taken as 2.5 bar and fixed. The number of revolutions per engine cycle,  $n_r$ , is needed to define  $P_e$  properly. In a four-stroke diesel engine, it is taken as two.  $Z$  denotes the number of cylinders, which was taken as six in this work. The volume displaced per cylinder,  $V_d$ , is calculated as follows [63]:

$$V_d = S(\pi B^2/4), \quad (2)$$

where  $B$  is the engine cylinder bore, and  $S$  denotes the cylinder stroke, taken as 107 mm and 124 mm, respectively, as indicated in Table 1.  $BMEP$  was predicted in the simulation as follows [63]:

$$BMEP = IMEP_{nominal} - FMEP, \quad (3)$$

where  $FMEP$  (bar) and  $IMEP_{nominal}$  (bar) denote the friction mean effective pressure and nominal indicated mean effective pressure, respectively. Sandoval and Heywood's friction model was preferred in the model to predict the  $FMEP$  [64]:

$$FMEP_{total} = (FMEP_{rotating}) + (FMEP_{reciprocating}) + (FMEP_{valvetrain}) + (FMEP_{auxiliary}). \quad (4)$$

In Formula (4), the effect of all rotating, reciprocating, valvetrain, and auxiliary components were considered for  $FMEP$  calculation.  $IMEP_{nominal}$  in Equation (3) was determined by adding  $IMEP_{gross}$  and  $PMEP$  (pumping mean effective pressure) [65]:

$$IMEP_{nominal} = IMEP_{gross} + PMEPE. \quad (5)$$

$IMEP_{gross}$  (gross indicated mean effective pressure) can be denoted as the power-producing potential of the cylinder without considering pumping and friction loss in the system.  $IMEP_{gross}$  and  $PMEPE$  are calculated through the variation of the in-cylinder pressure during closed and open cycles, respectively [65]:

$$IMEP_{gross} = \int \left( \frac{PdV}{V_d} \right)_{\text{closed cycle}}, \quad (6)$$

$$PMEPE = \int \left( \frac{PdV}{V_d} \right)_{\text{open cycle}}. \quad (7)$$

In a diesel engine system, high  $IMEP_{gross}$ , low  $PMEPE$ , and low  $FMEPE$  are desired to improve fuel efficiency. The model utilizes brake power ( $P_e$ ) and diesel fuel rate to determine the brake-specific fuel consumption ( $BSFC$ ) [63].

$$BSFC = \dot{m}_f / P_e, \quad (8)$$

where  $\dot{m}_f$  (g/h) represents the diesel fuel flow rate needed to maintain constant *BMEP*. Lastly, engine breathing capability—namely, volumetric efficiency ( $\eta_{vol}$ )—is calculated in the model using the expression below [63].

$$\eta_{vol} = \left( \frac{2\dot{m}_{ia}10^3}{30V_d N \rho_{ia}} \right), \quad (9)$$

where  $\rho_{ia}$  denotes the density of the fresh air charged through the intake ports. In Equation (9),  $\dot{m}_{ia}$  (g/h) represents the flow rate of intake air.

The in-cylinder combustion is defined via use of two-part Wiebe function, which mainly includes two distinct parts, namely, premixed and diffusion periods [66]. The fraction of the burned mass for the first period is calculated using Equation (10).

$$m_{frac,premixed} = 1.0 - \left( 1 - \left( \frac{\theta}{\theta_b} \right)^{C_1} \right)^{C_2}. \quad (10)$$

For the latter period, the fraction is obtained with

$$m_{frac,diffusion} = 1.0 - \exp^{-A \left( \frac{\theta - \Delta}{\theta_b - \Delta} \right)^{M+1}}. \quad (11)$$

The parameters in Equations (10) and (11)— $C_1$ ,  $C_2$ ,  $A$  and  $M$ —are taken as 2.5, 2500, 6.0, and 0.1, respectively. The interval between premixed and diffusion phases, namely,  $\Delta$ , is defined as 0.0.

The Annand heat transfer model is utilized to define the heat transfer per unit area, which is given as follows [67]:

$$\frac{dQ}{A} = h(T_{gas} - T_{wall}) + C(T_{gas}^4 - T_{wall}^4). \quad (12)$$

The parameter  $C$  in Equation (12) is taken as  $4.29 \times 10^{-9}$ . The convective heat transfer coefficient,  $h$ , is calculated using the following formula:

$$h = \frac{A Re^B k}{B_{cyl}}, \quad (13)$$

where  $k$  represents the thermal conductivity of the fluid, and  $Re$  is the Reynolds number. The parameters,  $A$  and  $B$ , are set for the open cycle period as 1.1 and 0.7 and for the closed cycle period as 0.2 and 0.8, respectively.

Unless an external component (such as an electrical heater) is present, exhaust gas energy remains as the sole energy source to heat up the EAT unit in a vehicle. Therefore, the heat transfer rate from the exhaust gas to EAT catalyst is critical to speed up the EAT warmup process. Three main parameters—namely, exhaust mass flow rate, exhaust temperature, and EAT catalyst bed temperature—determine how high or how low the energy transfer occurs between the exhaust unit and the EAT system. The heat transfer rate concerning those parameters can be defined using the relation below [68].

$$\dot{Q}_{transfer} = \dot{m}_{exhaust}^{4/5} \times C_p \times (T_{exhaust} - T_{EAT\ catalyst\ bed}), \quad (14)$$

where the heat transfer rate is denoted by  $\dot{Q}_{transfer}$ ,  $T_{exhaust}$  is the engine-out gas temperature at the EAT inlet, the EAT bed temperature is represented by  $T_{EAT\ catalyst\ bed}$ , and the flow rate through the EAT unit is illustrated with  $\dot{m}_{exhaust}$ .  $C_p$  is the exhaust heat capacity. The heat transfer calculation using Equation (14) should be seen as an approximation before obtaining the actual results through experimental work. However, it should also be noted that the relationship allows one to consider the effect of instantaneous EAT bed temperature and easily compare the potential of many different engine-dependent thermal

management methods. Those comparisons can enable reduced experimental work and, thus, cost-effectiveness.

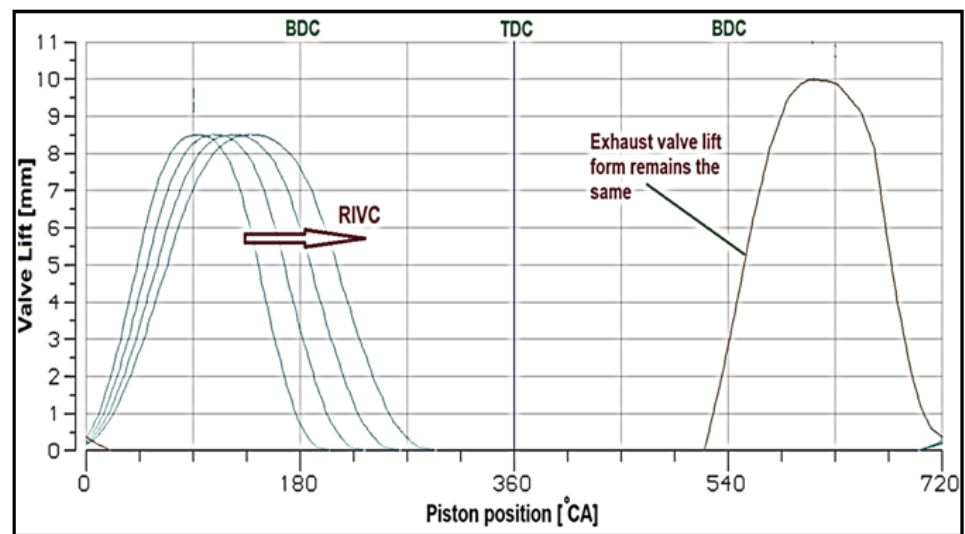
The model in Figure 1 was validated in a previous study [36] with the exhaust temperature results of an experimental study using IVC timing actuation [47]. It was proven to be highly beneficial, particularly to enhance diesel exhaust temperature above 250 °C in a low-load operation zone. IVC timing modulation elevates the exhaust temperature by decreasing the AFR and, thus, lowers the mass flow rate at the after-treatment inlet. Considering the significant role of the exhaust flow rate on EAT warmup, this strategy is not that effective for the get-warm period of the EAT systems. Moreover, unlike IVC timing control in [36], the model also exhibited highly promising results for EAT warmup through actuation of EVO timing in a previous analysis [48]. However, in this case, it caused considerable fuel inefficiency, thus increasing operation costs, as well as NOx and PM rates, until EAT warmup is maintained. Contrary to the aforementioned studies, the objective in this work is to improve the tradeoff between *BSFC* and EAT warmup via modulating both IVC and EVO timings. In fact, this study can be considered as a follow-up to [36,48] aimed at overcoming the negative effects of these earlier analyses. The RIVC + DEVO combined mode did not decrease exhaust mass flow rate as dramatically as either EIVC alone or RIVC alone. This is probably because, unlike IVC-based modulation, modified exhaust valve lift forms do not directly affect the airflow rate in the system. The combined mode also necessitates a lower fuel penalty. Therefore, simultaneous and reasonable control of the intake and exhaust valve lift profile is more effective to keep both the temperature and the mass flow rate at the after-treatment inlet at high levels, thereby ensuring rapid EAT warmup.

### 2.3. Application of RIVC + DEVO Combined Technique

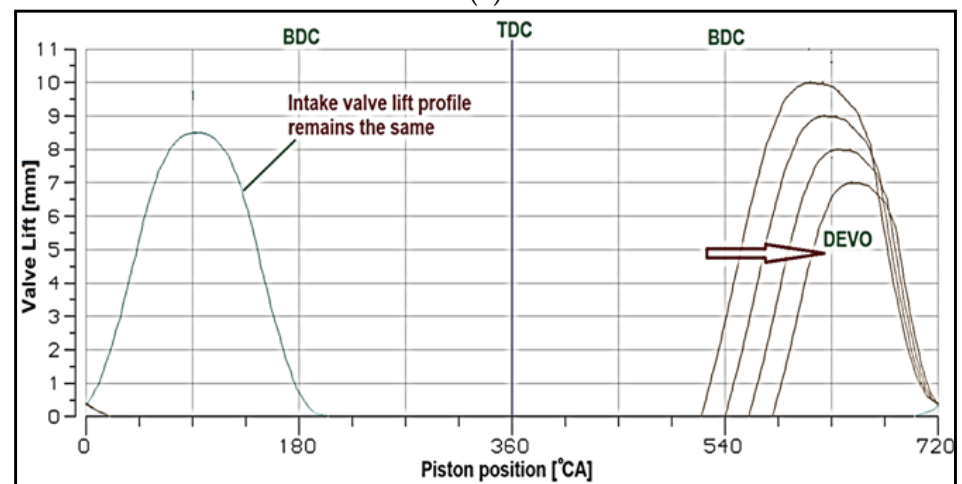
In the study, not only is IVC timing modulated, but EVO timing is also actuated. The simultaneous delay of these two timings was the focus of the work. However, the delay of the IVC alone (RIVC) and EVO alone (DEVO) cases was also considered for comparison. The valve lift forms in traditional RIVC alone and DEVO alone cases are illustrated in Figure 2a,b. Only intake closure was delayed in the RIVC alone mode, with a similar exhaust valve lift form to the nominal mode. Retarding the IVC extended the total intake opening duration, causing a relatively smoother rise and fall of intake valve lifts—less sharp lifts—compared to nominal mode, as seen in Figure 2a. Unlike the RIVC alone mode, the DEVO alone mode shortened the total exhaust opening duration without affecting the intake valve lift profile in Figure 2b. This led to relatively sharper increases and decreases in exhaust valve lifts compared to the nominal mode. The exhaust valve maximum lift was reduced in DEVO mode to prevent a possible piston-valve crash, which is undesirable in any VVT mode. In contrast to the single-VVT modes, Figure 3 demonstrates the retardation of both IVC and EVO timings, namely, the RIVC + DEVO combined mode. This mode affected both the intake and the exhaust valve lift forms. Not only was intake opening lengthened due to RIVC, but exhaust opening was also contracted due to DEVO. Overall, unlike the aforementioned single-handed modulations, the RIVC + DEVO combined mode can be seen as a double-handed modulation, coupling IVC and EVO timings. Table 3 summarizes the steps in all VVT modes, including the nominal mode and increments in each mode, to achieve the extreme case.

Valve timing actuation has a direct influence on the flow into and out of the cylinder. Therefore, cylinder performance parameters—particularly engine-out temperature for this work—can be easily modulated through the reasonable control of valve lift profiles. However, during this modulation, *BSFC* can exceed engine design limits, which is undesirable. In this work, the RIVC + DEVO combined method is proposed (see Figure 3) to improve *BSFC* while the EAT works above 250 °C in an effective manner. In the next section, the technique is compared with the RIVC alone and DEVO alone cases (single-VVT applications) to show the benefits of the proposed method for engine performance and EAT warmup.





(a)



(b)

Figure 2. (a) Application of RIVC alone method. (b) Application of DEVO alone method.

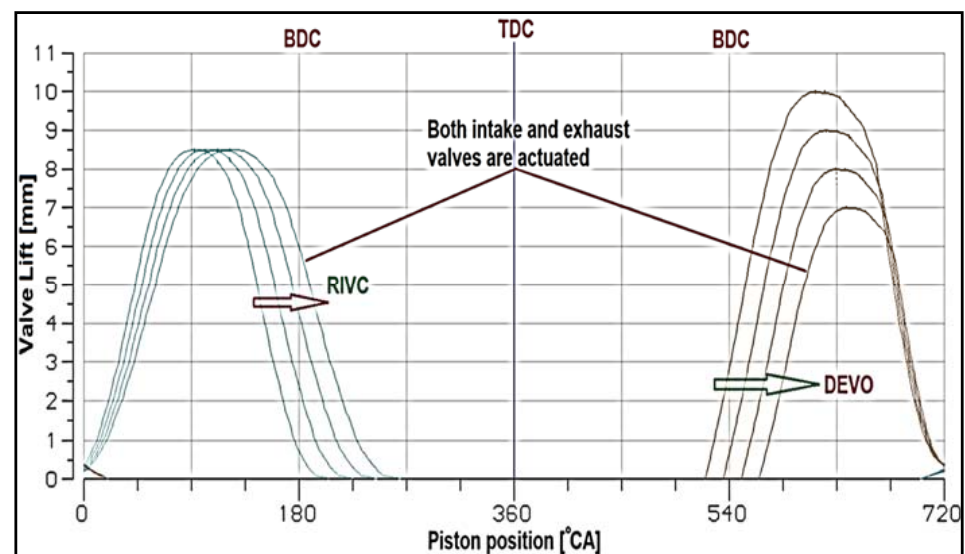


Figure 3. Application of RIVC + DEVO combined method.

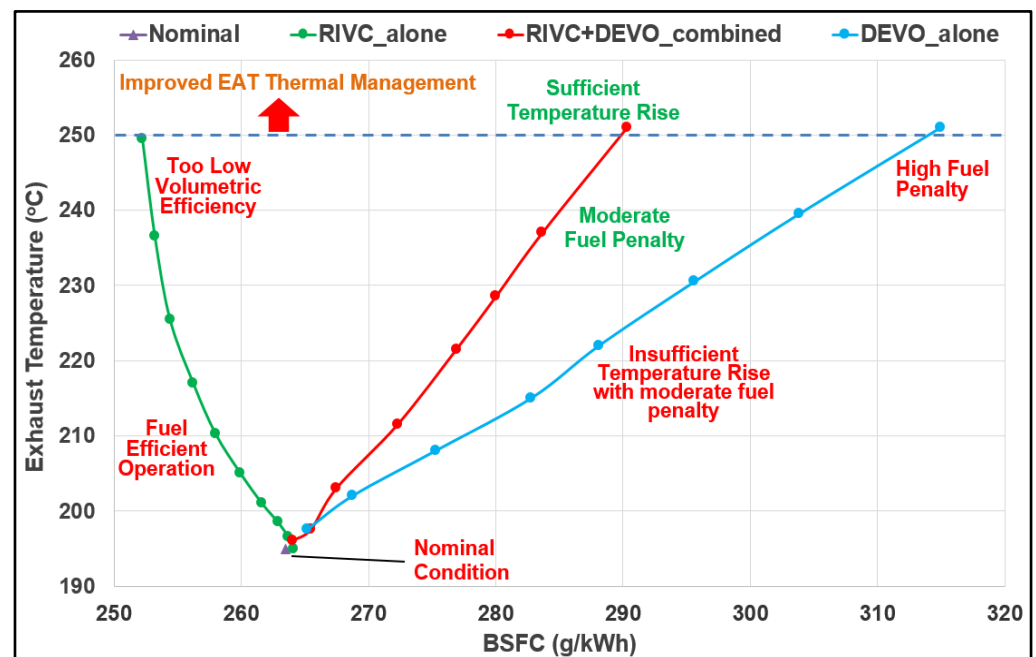
**Table 3.** Steps for RIVC alone, DEVO alone, and RIVC + DEVO combined modes.

Method	Engine Parameter	Nominal Case	Increment (°CA)	Extreme Case
RIVC	IVC (°CA ABDC)	25	+10	125
DEVO	EVO (°CA BBDC)	20	−10	−70
RIVC +	IVC + EVO combined	(25)	(+10)	(85)
DEVO		(20)	(−10)	(−60)

### 3. Results and Discussion

#### 3.1. Effects on EAT Inlet Temperature and Exhaust Flow Rate

The temperature at the after-treatment inlet is the primary factor for an effective TWC unit in an automotive engine system. Therefore, the impact of any engine-based technique on engine-out temperature is significant for researchers and engine producers. The effects of RIVC, RIVC + DEVO combined, and DEVO on turbine-out exhaust temperature are shown in Figure 4. Engine load was held constant by modifying the fuel injection rate as the IVC and EVO timings were altered in the model.

**Figure 4.** Changes in exhaust gas temperature and BSFC using different techniques.

It can be seen in Figure 4 that nominal condition had an exhaust temperature (195 °C) much lower than the threshold temperature (~250 °C) where enhanced EAT operation was achieved. Obviously, temperatures close to or above 250 °C are ideal for effective NOx reduction [15,18]. Therefore, the nominal condition had the lowest potential to reduce NOx as the catalysts inside the SCR system could only be increased up to 195 °C in this mode. The aim of any method is to move this low-temperature operating point above the 250 °C temperature line and enable high potential for NOx minimization.

The RIVC, RIVC + DEVO combined, and DEVO methods were all applied until the turbine-out temperature exceeded 250 °C (see Figure 4). All strategies were capable of maintaining improved thermal management of the EAT unit in the system. However, every strategy seemed to act in a different manner in terms of BSFC during valve timing modulations.

RIVC enhanced both exhaust temperature and *BSFC* (Figure 4). Similar to previous studies [41,47], it was advantageous to use RIVC at low loads as it had the potential to maintain fuel-saving performance through reduced airflow rate. The improvement in temperature seemed to be insignificant at less retarded IVC cases due to the relatively insignificant reduction in air charge into the cylinders (see Figure 5). However, at moderately and highly retarded IVC cases, the temperature improvement accelerated as the volumetric efficiency ( $\eta_{vol}$ ) and, thus, in-cylinder charge considerably decreased (Figure 5).

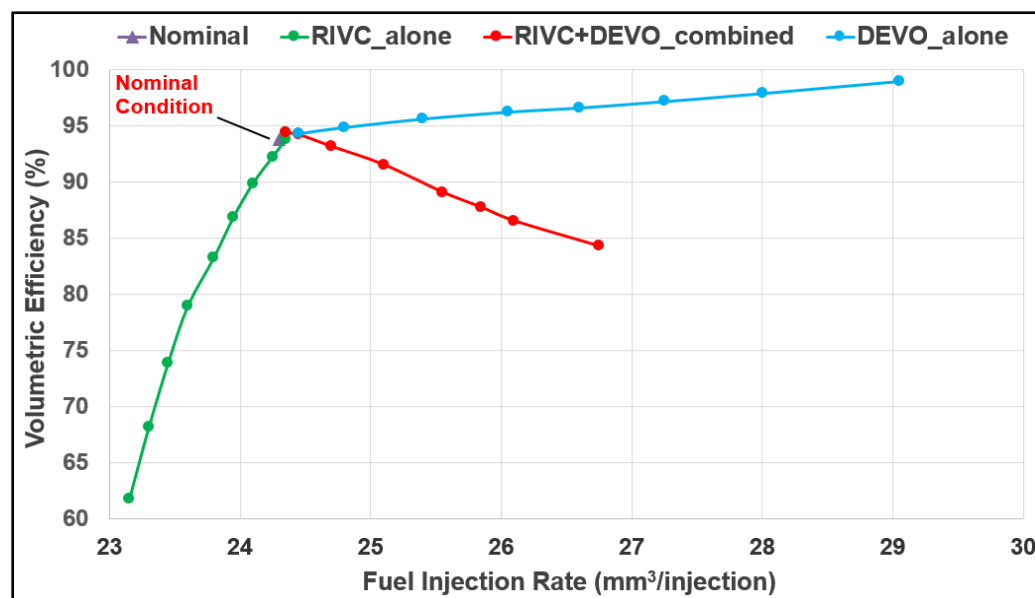


Figure 5. Changes in volumetric efficiency and fuel injection rate using different techniques.

Unlike the RIVC method, the DEVO and RIVC + DEVO combined techniques necessitated higher fuel consumption to keep engine power constant (see Figure 4). The fuel penalty is considerably high in DEVO mode as a high temperature ( $T_{exhaust} > 250\text{ }^{\circ}\text{C}$ ) is desired in the system. Keeping the fuel penalty at low levels in this mode was not a solution since the exhaust temperature could barely move above  $220\text{ }^{\circ}\text{C}$  in these cases, which was inadequate to maintain effective EAT. Nevertheless, DEVO is a proven approach to increase engine-out temperature at low loads [50]. Combining DEVO with RIVC still imposed a fuel consumption penalty (see Figure 4), but not as high as the DEVO method. For a similar *BSFC* increase (moderate fuel penalty), the exhaust temperature was enhanced in the RIVC + DEVO combined mode by almost  $30\text{ }^{\circ}\text{C}$  more compared to the DEVO mode. This temperature difference had the advantage of maintaining an efficient EAT and, thus, low NOx rates with improved *BSFC* in the system.

The increase in *BSFC* in the DEVO alone and RIVC + DEVO combined modes was certainly disadvantageous compared to the RIVC alone strategy. However, as shown in Figure 5, those two fuel-inefficient methods did not affect  $\eta_{vol}$  as dramatically as the RIVC alone method when the exhaust temperature exceeded  $250\text{ }^{\circ}\text{C}$ . The slight reduction in  $\eta_{vol}$  in the RIVC + DEVO combined mode was due to the moderate use of RIVC in this mode, unlike its aggressive use in the RIVC alone mode. DEVO alone did not affect  $\eta_{vol}$  in a negative manner. In fact, in this mode, there was a slight increase in  $\eta_{vol}$ , probably due to the rapid mass discharge and the increase in exhaust flow and turbine speed. As a result, RIVC had the disadvantage of having the lowest  $\eta_{vol}$  (see Figure 5) and, thus, probably the lowest potential to enhance EAT warmup among all techniques. It can be deduced that high temperature was a must, albeit not sufficient for rapid EAT warmup. Considering the upward and downward changes in  $\eta_{vol}$  at different valve modulations (see Figure 5), a similar change in exhaust flow rate was observed using different VVT modes (Figure 6).

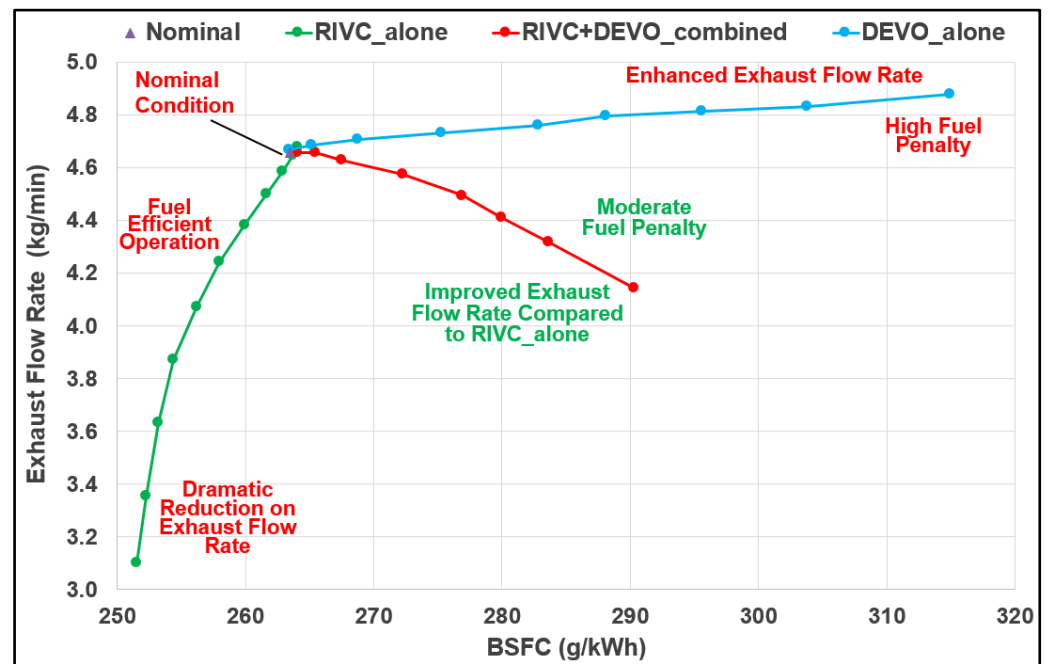


Figure 6. Changes in exhaust gas flow rate and *BSFC* using different techniques.

As the  $\eta_{vol}$  is the dominant parameter affecting engine-out flow rate in a diesel engine system, the plot of exhaust flow rate in Figure 6 was almost identical to that of  $\eta_{vol}$  in Figure 5. Some slight differences between the plots were due to the rise or fall in fuel injection rate in Figure 5, which is regarded as a secondary parameter affecting exhaust flow rate. Since DEVO alone caused the highest increase in fuel injection rate and had a negligible effect on  $\eta_{vol}$ , it enabled the highest exhaust flow rate at the EAT inlet (see Figure 6).

Unlike the DEVO alone mode, the RIVC alone and RIVC + DEVO combined modes led to decreased exhaust flow rates at the turbine exit (see Figure 6). The reduction observed for the RIVC alone mode was due to the decrease in fuel injection rate and  $\eta_{vol}$  in Figures 4 and 5, respectively. The RIVC + DEVO combined mode led to a relatively lower increase in *BSFC* compared to DEVO alone but somewhat reduced  $\eta_{vol}$  (Figure 5). Thus, it had a negative contribution to the exhaust flow rate (Figure 6), albeit much closer to the nominal condition, and not as suddenly reduced as for RIVC alone, which is advantageous. The change in  $\eta_{vol}$  and fuel injection rate also affected AFR, as shown in Figure 7.

AFR had a decreasing trend using all strategies (Figure 7). However, there was an evident reduction in AFR when RIVC alone was adopted in the system. This stemmed from the sudden reduction in airflow rate in this mode as  $\eta_{vol}$  was reduced by almost one-third (Figure 5). The improvement in fuel injection rate in the RIVC alone mode was negligible compared to the change in airflow rate and, thus, did not have a significant effect on AFR. Comparing Figures 4 and 7, it can be deduced particularly for RIVC alone mode that low AFR was the key element to achieve an exhaust temperature above 250 °C.

AFR in the DEVO alone mode decreased (Figure 7) although the airflow rate increased slightly compared to the nominal condition (Figure 6). Unlike the RIVC alone mode, AFR in the DEVO alone mode was reduced not due to the low airflow rate, but the steadily rising high fuel injection rate, as indicated in Figure 5. The difference between these two modes can be better understood by comparing Figures 4 and 6. Both modes attained the threshold exhaust temperature (~250 °C). DEVO alone had a high in-cylinder mass to warm up, thus necessitating a high *BSFC* (minor reduction in AFR). However, RIVC alone was fuel-saving as it had a much lower mass to be heated (major reduction in AFR). AFR in the RIVC + DEVO combined technique remained between

these two extreme cases (Figure 7) since it did not allow a noticeable reduction in  $\eta_{vol}$  or a considerable rise in fuel penalty, as evident in Figure 5. The trend of AFR in the combined mode was predicted to approach the trend of AFR in the RIVC alone mode, as IVC was retarded more and EVO was delayed less in this mode. Otherwise, it tended to approach the trend of AFR in the DEVO alone mode. Moving the operating point closer to the DEVO alone mode in Figure 7 was limited by the sharp fuel penalty rise in Figure 4 and the possible rapid increase in NO<sub>x</sub> rates due to high inefficiency. High EGR rates are required to prevent such undesirable NO<sub>x</sub> rates, which generally cause high soot flow rates. However, directing the operating point closer to the RIVC alone mode is more practical as the fuel penalty rise is relatively less challenging; thus, a possible moderate increase in NO<sub>x</sub> and soot rates can be avoided by using moderate EGR rates.

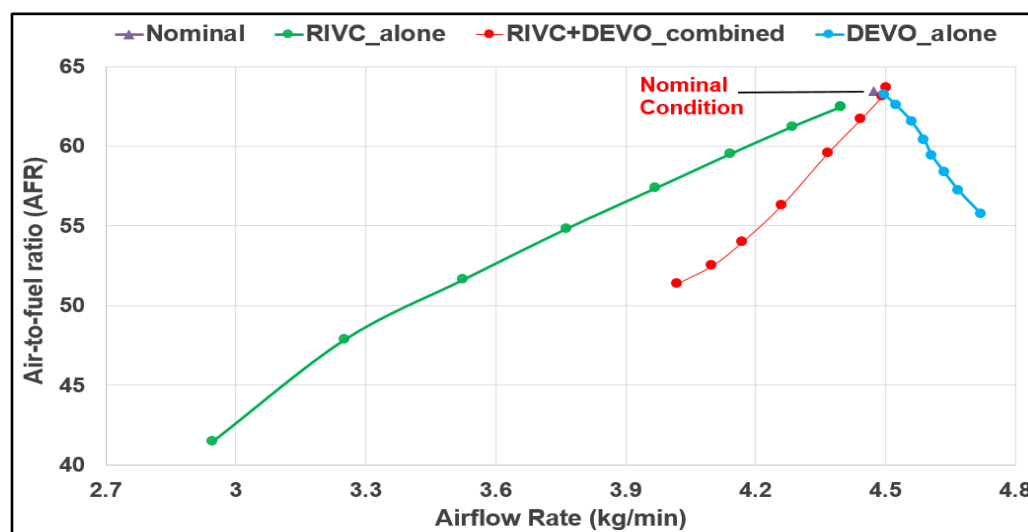


Figure 7. Changes in AFR and total airflow rate using different techniques.

### 3.2. Effects on Engine Thermal Efficiency, Heat Loss, and Flow Rates at Ports

This section discusses the engine performance parameters affecting thermal efficiency, as well as the intake and exhaust flow rates at ports. EAT warmup mostly requires a tradeoff between the engine thermal efficiency and exhaust energy improvement at the EAT inlet. Therefore, an assessment of the thermal efficiency and flow rates is important when proposing a new method for rapid EAT warmup in an HD diesel engine system.

At first, unlike the previous plots, the effect of different VVT modes on  $BMEP$  is examined in Figure 8 without altering the fuel injection rate (FIR) to keep the engine power fixed. Instead, FIR is held constant and  $BMEP$  is allowed to change while IVC or EVO is retarded to yield a high exhaust temperature in the system.

The system steadily produced lower  $BMEP$  when the DEVO alone or RIVC + DEVO combined mode was implemented (Figure 8). This was expected since these two modes needed additional fuel consumption to maintain constant engine load, as indicated in Figure 5. The reduction in  $BMEP$  in DEVO alone mode was considerable (Figure 8). The engine was forced to produce lower than 1.9 bar  $BMEP$  under the extreme use of DEVO, far from that achieved in nominal conditions (2.5 bar). This undesirable working condition could be attributed to the high pumping loss ( $PMEP$ ) in DEVO mode, as demonstrated in Figure 9. Increased  $PMEP$  caused a significant reduction in brake thermal efficiency (BTE) in Figure 9, since  $IMEP_{power}$  (power producing potential of the engine) needed to constantly increase in DEVO mode to maintain the engine load. Unlike DEVO mode, the RIVC mode improved the  $BMEP$  (Figure 8). This is because RIVC resulted in lower  $PMEP$  (Figure 9); thus, lower  $IMEP_{power}$  was adequate to achieve similar engine load in this mode.

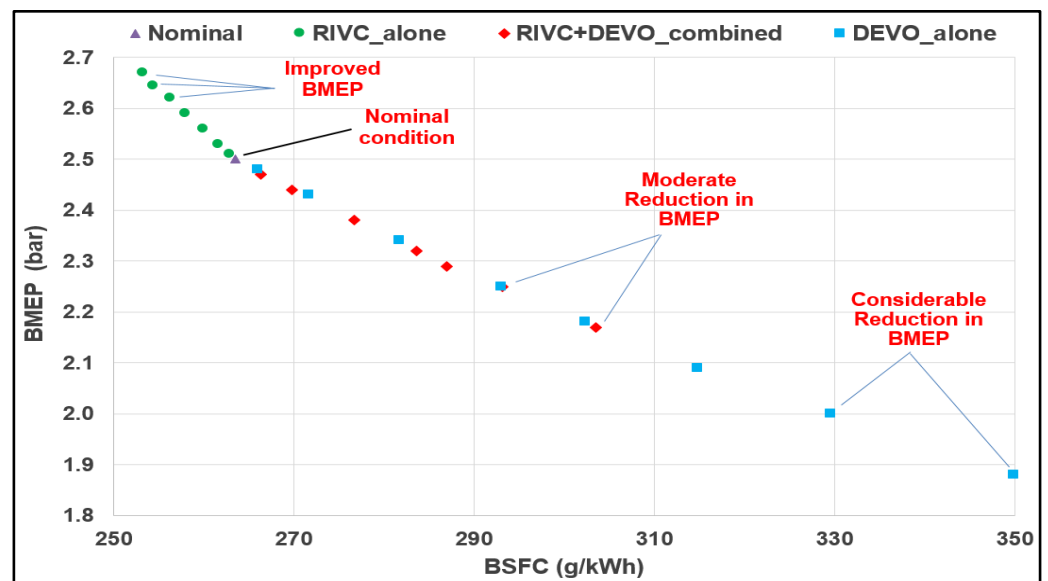


Figure 8. Changes in  $BMEP$  and  $BSFC$  for constant FIR using different techniques.

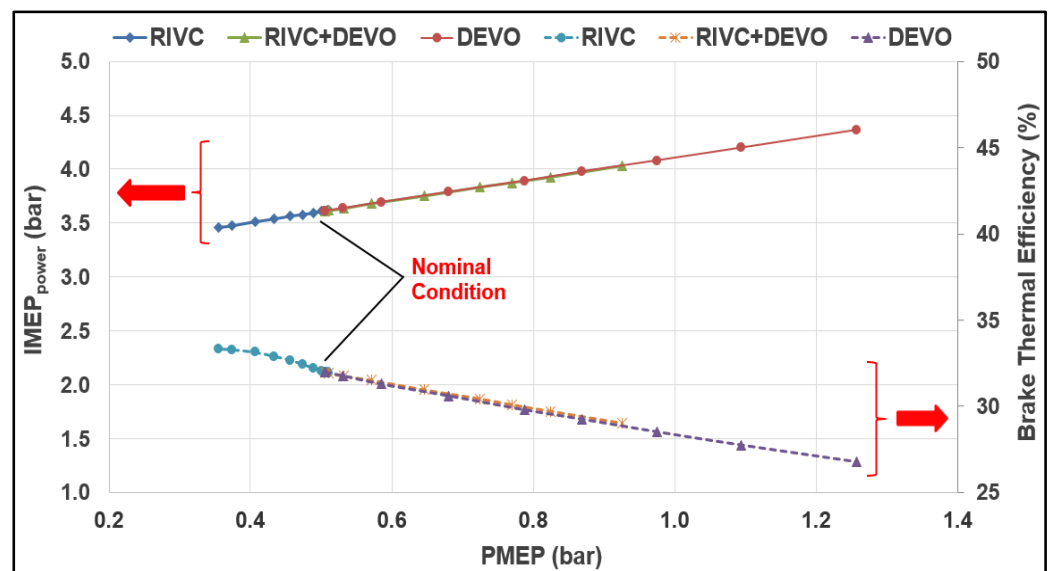


Figure 9. Changes in  $IMEP_{power}$  and  $PMEP$  using different techniques.

The RIVC + DEVO combined mode led to a moderate reduction in  $BMEP$  (Figure 8). Even in the extreme use of the RIVC + DEVO technique,  $BMEP$  remained close to 2.2 bar, which was hardly achieved in the moderate use of DEVO alone. This was due to the improving effect of the partial use of RIVC on  $PMEP$  in combined mode (Figure 9). The reduced  $PMEP$  in the RIVC + DEVO combined mode enabled improved BTE compared to DEVO alone (Figure 9). This fuel-efficient operation could be attributed to the lower fuel penalty (and, thus, lower  $IMEP_{power}$ ) needed in this mode to run the engine at 2.5 bar  $BMEP$ . The difference in  $PMEP$  between the methods (see Figure 9) could be better realized when the behavior of the in-cylinder pressure during the exhaust phase in the nominal mode and extreme mode of each VVT technique (as in Table 3) was examined and compared (see Figure 10).

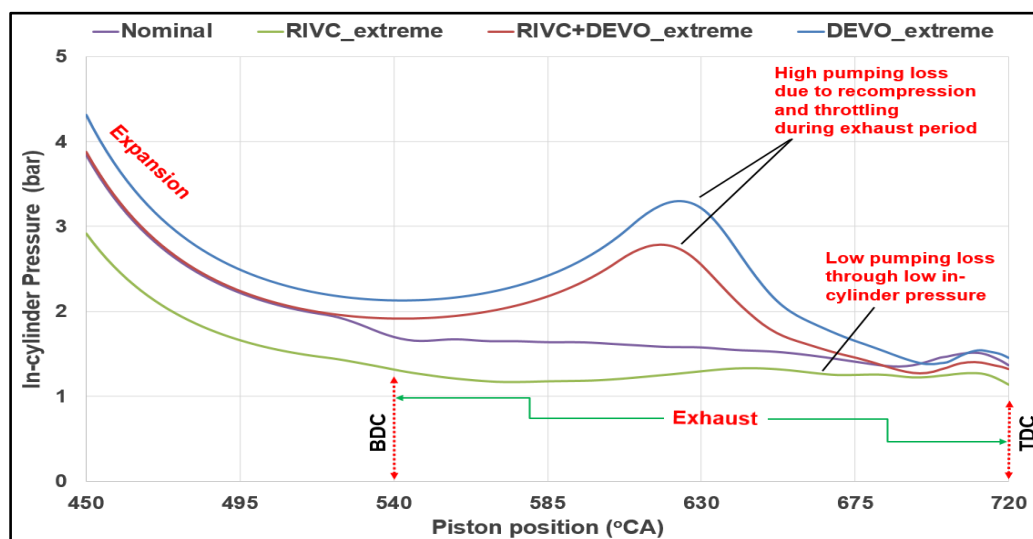


Figure 10. Behavior of in-cylinder pressure during exhaust period using different techniques.

It can be seen in Figure 10 that the in-cylinder pressure before the exhaust phase was the highest and the lowest in the DEVO extreme and RIVC extreme modes, respectively. The pressure was also very similar in the nominal and RIVC + DEVO modes during the pre-exhaust phase. The low pressure in the RIVC extreme case was due to the reduced effective compression ratio as a function of engine operation with low  $\eta_{vol}$ , as illustrated in Figure 5. During the exhaust phase (Figure 10), the RIVC extreme mode still maintained the pressure at low levels and completed the phase with the lowest in-cylinder pressure among all techniques. In fact, this is the reason why only the RIVC method improved the pumping loss and the BTE (Figure 9). It can be deduced from Figure 10 that the aggressive use of RIVC (i.e., RIVC extreme) was advantageous due to the low pressure and less challenging exhaust removal in the system.

Contrary to the RIVC extreme mode, the DEVO extreme and RIVC + DEVO extreme modes caused an increase in in-cylinder pressure during the exhaust phase (Figure 10). The pressure in the nominal mode remained below these two modes and close to the RIVC extreme mode, as it featured a similar EVO timing to the RIVC extreme mode. As soon as the expansion phase was completed (Figure 10), the in-cylinder pressure in the DEVO extreme and RIVC + DEVO extreme modes differed greatly from that in the nominal and RIVC extreme modes. The pressure started to elevate particularly due to the recompression of the in-cylinder exhaust gas in these modes. The pressure increase in the DEVO extreme mode compared to the RIVC + DEVO extreme mode was higher, partially due to the more retarded EVO timing, which resulted in a higher recompression of in-cylinder flow. Another contributing factor to the pressure increase in the DEVO extreme mode was the higher total mass trapped inside the cylinder due to the unmodified intake valves, which did not allow for any reduction in in-cylinder airflow during operation. The RIVC + DEVO extreme mode utilized RIVC to lower the in-cylinder mass, thus resulting in a relatively lower pressure increase and pumping loss (Figure 10). In both DEVO-dependent modes, a sudden expansion of exhaust gas was observed in the second half of the exhaust phase. This can be attributed to the release of the accumulated in-cylinder energy due to late EVO in these modes. The changes in in-cylinder air charge and pressure also affected the in-cylinder temperature (Figure 11).

During the compression phase (Figure 11), the RIVC extreme mode exhibited the lowest temperature increase due to the reduced effective compression ratio. The DEVO extreme and nominal cases had a high in-cylinder temperature due to compression of the high in-cylinder mass. The RIVC + DEVO extreme mode was intermediate between the aforementioned extreme cases since it only allowed for a partial reduction in the effective compression ratio. The fuel injection timing (stated as 3 °CA BTDC in Table 1) was the

same in all modes. Therefore, the increase in in-cylinder temperature during combustion occurred at approximately the same piston position in all modes. Since the RIVC alone mode had the minimum AFR, as illustrated in Figure 7, the in-cylinder temperature increased the most during heat release in the RIVC extreme mode (Figure 11). The DEVO extreme and RIVC + DEVO extreme modes had comparable in-cylinder temperatures. However, the in-cylinder temperature increased in these modes, not due to a radical reduction in AFR as seen in the RIVC alone mode (Figure 7), but due to increases in the fuel penalty and engine inefficiency (Figure 9). The in-cylinder temperature in the nominal mode remained the lowest during combustion (Figure 11) as it operated with the highest AFR among all methods.

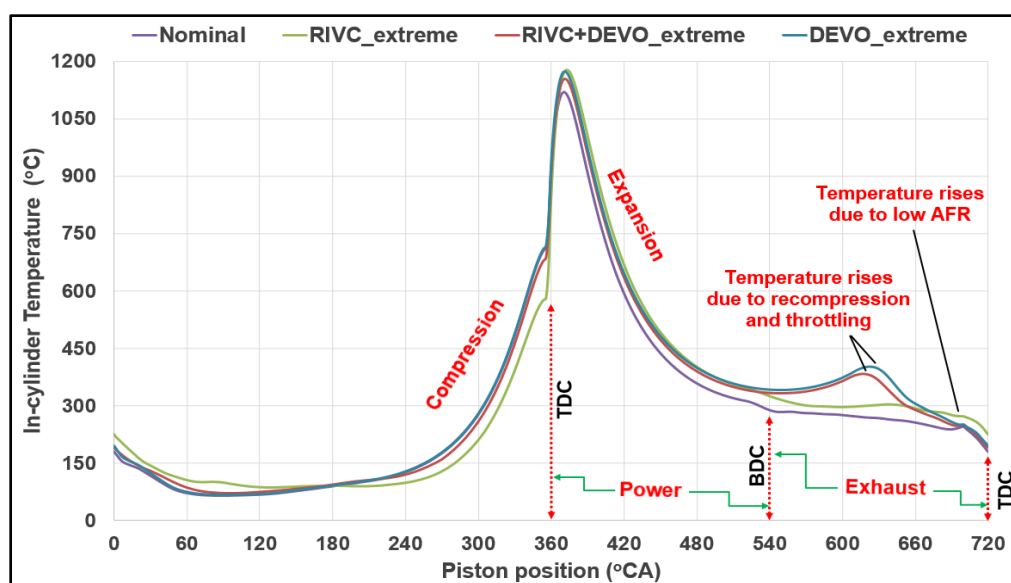


Figure 11. Behavior of in-cylinder temperature during cycle using different techniques.

Following the power phase (Figure 11), in the exhaust phase, the in-cylinder temperature in each mode behaved very similarly to the in-cylinder pressure change in each mode (Figure 10). The recompression and throttling in the DEVO-based modes increased the temperature of the in-cylinder burnt gas before the flow through the exhaust port and, consequently, through the EAT system. The RIVC extreme mode already exhibited high temperature during expansion and also maintained it at high levels during the exhaust phase. The nominal mode is the most disadvantageous (Figure 11) since the temperature even fell below 250 °C during the exhaust period. Considering that the gas flowed through the turbocharger, before expanding in the turbine and losing more heat, the nominal mode—unlike the VVT modes—definitely could not meet the light-off temperature requirements of the EAT system. The temperature differences illustrated in Figure 11 resulted in some considerable engine heat loss using different techniques (Figure 12).

There was no significant change in cylinder heat loss at slightly retarded IVC cases using the RIVC alone mode (Figure 12). This is because the change in the mean in-cylinder temperature was negligible in these cases. However, with moderate and aggressive use of RIVC in this mode, the mean in-cylinder temperature increased rapidly due to the maintenance of a particularly high temperature during the power and exhaust phases (Figure 11). The increase in cylinder heat loss was limited in the RIVC alone mode compared to other modes due to the low in-cylinder airflow (Figure 7). A lower in-cylinder mass resulted in less cylinder heat loss (Figure 12), which was highly beneficial to achieving the fuel-efficient performance of the RIVC alone mode (Figures 4 and 6).



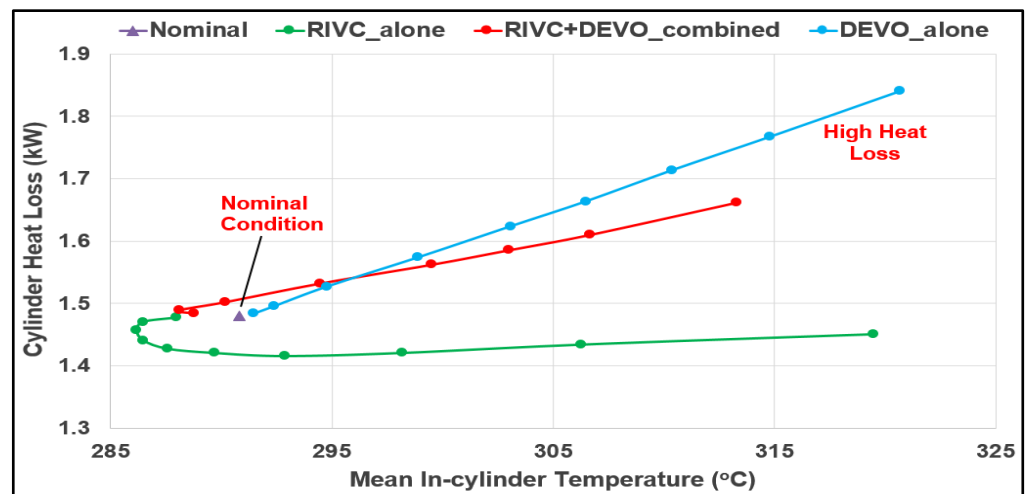


Figure 12. Changes in cylinder heat loss and mean in-cylinder temperature using different techniques.

The DEVO alone and RIVC + DEVO combined modes acted quite differently from the RIVC alone mode (Figure 12). The increase in heat loss using these modes was mainly attributed to the high in-cylinder temperature during the expansion and exhaust periods, as illustrated in Figure 11. DEVO alone resulted in the highest heat loss since it featured the highest in-cylinder mass (Figure 7). The heat loss in the RIVC + DEVO combined mode was somewhat less considerable due to the lower air charge and reduced fuel penalty compared to the DEVO alone mode. Figure 13 illustrates how the in- and out-of-cylinder flows varied at ports using different modes, thus affecting cylinder heat loss (Figure 12).

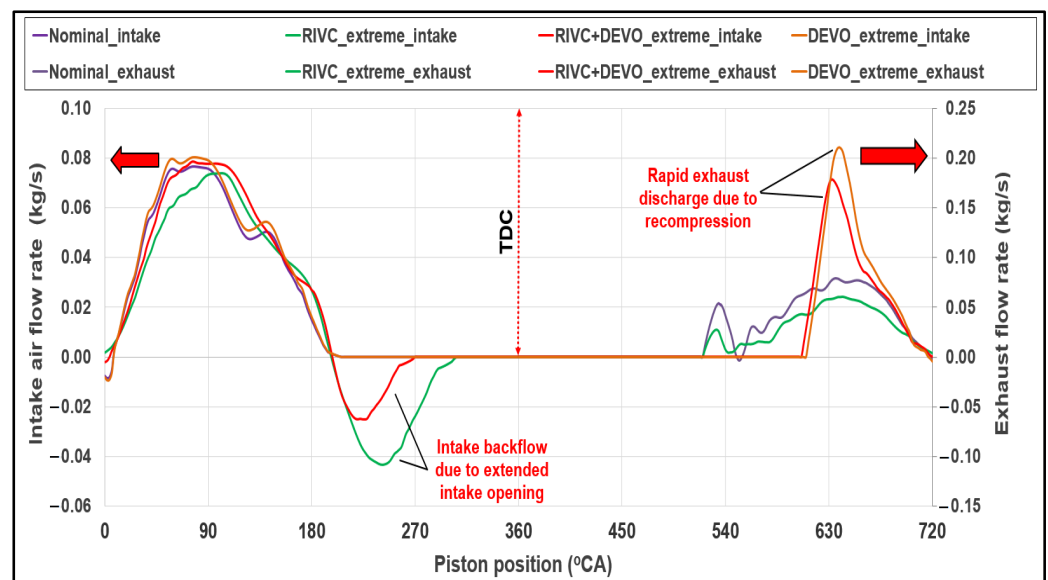


Figure 13. Behavior of intake air and exhaust flow rates at ports using different techniques.

It can be seen in Figure 13 that there was no essential difference in airflow rate at the intake port between the nominal and DEVO extreme modes. This is because these modes were performed with the same intake valve lift profile. The slight increase in air charge in the DEVO extreme mode could be attributed to the rapid increase in exhaust flow rate (Figure 13) due to the recompression of in-cylinder mass (Figure 10). This recompressed and increased in-cylinder energy led to a sudden release of exhaust gas, forcing the turbine to work more effectively; thus, more air could be inducted into the cylinders. However, the exhaust flow rate through the exhaust port in the nominal mode was not as rapid as that in

the DEVO extreme mode. Nevertheless, the duration of exhaust discharge was extended in the nominal mode, thus yielding a comparable total exhaust flow rate (Figure 6).

Unlike the nominal and DEVO extreme modes, the RIVC extreme and RIVC + DEVO extreme modes caused a considerable change in the intake airflow rate (Figure 13). The intake flow rate behavior was relatively similar until the nominal IVC timing (25 °CA ABDC) in all modes. As the piston motion was downward during that period, all cylinders in all modes could charge air at high or low levels depending on the valve lift profile. However, unlike the nominal and DEVO extreme modes, the intake valve was still open in the RIVC extreme and RIVC + DEVO extreme modes beyond the nominal IVC timing. The piston motion was upward during those timings (compression phase); thus, some portion of the in-cylinder charge was directed outward—through the intake port—in these modes due to the late IVC (Figure 13). The backflow of fresh air at the intake port was the reason for the decline in  $\eta_{vol}$  in the RIVC alone and RIVC + DEVO combined modes (Figure 5). The reverse intake flow was more meaningful in the RIVC extreme mode (Figure 13) due to the higher delay of IVC timing compared to the RIVC + DEVO extreme mode. The reduced intake flow and improved fuel consumption in the RIVC-dependent methods led to reduced exhaust flow rates at the exhaust port compared to the nominal and DEVO extreme modes (Figure 13).

### 3.3. Comparison of the Techniques with Regard to the Potential to Improve Exhaust Energy and EAT Warmup

This section aims to explicitly discuss the effect of the VVT techniques of interest on exhaust energy and EAT warmup. In a conventional automotive engine system, an external heating tool is not generally placed to heat the EAT unit due to high cost. Therefore, the exhaust energy at the EAT inlet is normally the main source of rapid catalytic converter warmup. Figure 14 displays the impact of each method on exhaust energy.

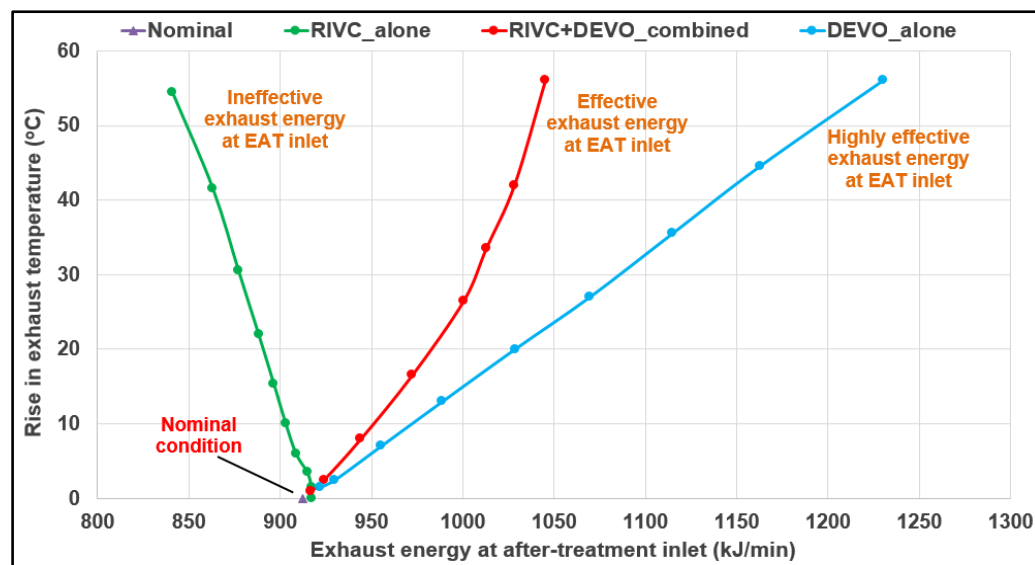


Figure 14. Exhaust energy at EAT inlet vs. rise in exhaust temperature using different techniques.

The total increase in exhaust temperature for each mode is also shown in Figure 14 to compare the trend of exhaust energy when an adequate temperature increase was achieved in all modes. There was a certain reduction in exhaust energy in the RIVC alone mode (Figure 14) due to the highly reduced exhaust flow rate (Figure 6). The RIVC alone mode enabled a further increase to 55 °C exhaust temperature. However, it was obviously inadequate to improve the exhaust energy at the EAT inlet. In contrast to the RIVC alone mode, the other techniques could noticeably enhance the exhaust energy (Figure 14). The DEVO alone mode was particularly outstanding (Figure 14), being superior to both the RIVC alone and the RIVC + DEVO combined modes due to the improvements in exhaust

temperature and exhaust flow rate, as indicated in Figure 6. The increase in exhaust energy in the RIVC + DEVO combined mode slowed down, especially during the moderate and aggressive use of the method, due to the delayed IVC timing and partial reduction in exhaust flow rate. Nevertheless, a comparable temperature rise could still be achieved (above 50 °C) with only half the fuel consumption penalty of the DEVO alone mode, as shown in Figure 4. The fuel-saving potential of this technique is likely to produce lower NO<sub>x</sub>, CO, and soot rates compared to the DEVO alone technique when the EAT is heated above the light-off temperature (~ 250 °C).

It can be seen in Figure 14 that both the exhaust temperature and the exhaust flow rate should be considered when determining how fast an engine-based technique can heat the EAT unit. Therefore, Equation (14) was utilized to establish a relative comparison of each method with respect to its potential to enhance EAT unit warmup. Equation (14) is a relatively simplified approximation for observing the heat transfer rates to the after-treatment system. However, it considers the dynamic temperature variation of the EAT system, thus representing a framework for comparisons of different approaches in a plot.

In transient operation, heat transfer rates change instantaneously along with the exhaust flow rates and exhaust temperatures. However, in steady operation—as in this study, with a constant engine *BMEP* of 2.5 bar—only  $T_{EAT\ catalyst\ bed}$  was in constant flux (the EAT unit was either heated by hot exhaust or cooled by cold exhaust). The exhaust flow rate and turbine-out temperature remained fixed. The EAT unit was assumed to work over a temperature range of [−50, 350 °C] considering operation in cold weather (cold start-up) and above light-off temperature (over 250 °C). Using Equation (14), the heat transfer rates ( $\dot{Q}_{transfer}$ ) from the exhaust gas to the EAT catalyst were calculated for several points in the aforementioned temperature range. Four different modes were considered in the analysis: nominal, RIVC extreme, RIVC + DEVO extreme, and DEVO moderate. Whereas the nominal mode worked with the valve timings given in Table 1, the RIVC extreme and RIVC + DEVO extreme modes worked with the extreme valve timings stated in Table 3. The DEVO extreme mode caused an undesirable fuel penalty (20%), as shown in Figures 4 and 6, which was impractical for accelerating EAT warmup. Therefore, it could not be suitably compared with the nominal, RIVC extreme, and RIVC + DEVO extreme modes. Thus, instead of the DEVO extreme mode, the DEVO moderate mode was used for the heat transfer rate comparisons. The delay of EVO timing was limited in the DEVO moderate mode to maintain the fuel consumption penalty at 10%. The RIVC + DEVO extreme mode had the same fuel penalty (10%); thus, comparing it with the DEVO moderate mode was more suitable than the DEVO extreme mode.

To simplify the comparison of  $\dot{Q}_{transfer}$  in each mode, the heat transfer rate in the nominal mode at a 0 °C EAT bed temperature was considered as 1.0. In other words, the heat transfer rate at this EAT bed temperature was set as the baseline in the nominal mode. All other heat transfer rates in all modes were normalized to this baseline. The normalized heat transfer rates for the nominal, RIVC extreme, RIVC + DEVO extreme, and DEVO moderate modes are presented in Figure 15.

The EAT unit could only be heated to a temperature where the heat transfer rate crossed the x-axis in Figure 15. In fact, these points corresponded to the “zero heat transfer” points for each mode, where  $T_{exhaust}$  was equal to  $T_{EAT\ catalyst\ bed}$ . An equilibrium was provided between the exhaust unit and the EAT system at these points. Above these points, the transfer rates were positive since the engine-out temperature can be maintained above the catalyst temperature ( $T_{exhaust} > T_{EAT\ catalyst\ bed}$ ). Obviously, it is desirable to have high heat transfer rates in this zone to shorten the EAT warmup time. In contrast, below these points (below the zero heat transfer line in Figure 15), the heat transfer rates were negative as the exhaust temperature remained below the catalyst temperature ( $T_{exhaust} < T_{EAT\ catalyst\ bed}$ ). The EAT unit would lose heat at these points; thus, low heat transfer rates are advantageous in this zone to slow the EAT cooling time.

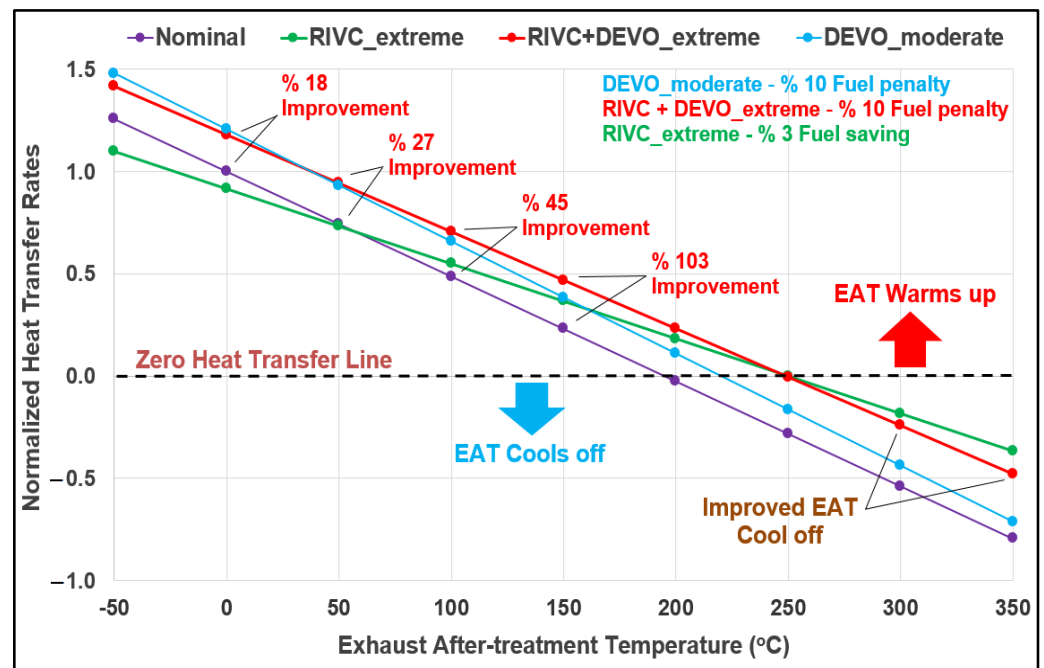


Figure 15. Comparison of the effect of different techniques on EAT catalyst warmup at 2.5 bar BMEP.

The nominal mode was the least effective for EAT warmup (Figure 15). This is mainly because it had the lowest exhaust temperature (195 °C) of all modes. The magnitude of the heat transfer rate was certainly reduced in the nominal mode since it had the lowest y-axis offset among all modes. The relatively high exhaust flow rate (compared to the RIVC extreme and RIVC + DEVO extreme modes) was also disadvantageous as it resulted in high negative heat transfer rates and, thus, accelerated EAT cool off. Overall, the nominal mode was not consistent with the get-hot or stay-hot periods of the EAT unit.

The RIVC extreme mode benefited from a high exhaust temperature (250 °C) and, thus, high y-axis offset (Figure 15). However, the slope of the heat transfer line, indicating how fast the related mode reached the heat transfer neutral point, was determined as a function of the exhaust flow rate, which was highly reduced in the RIVC alone mode (Figure 6). Therefore, similarly to the nominal mode, the RIVC extreme mode was not preferred to enhance the get-warm period of the EAT system. Nevertheless, it may be preferred during the stay-warm period due to the enhanced EAT cool off via reduced exhaust flow rate, as well as the up to 3% fuel-efficient operation (see Figures 4 and 9).

The DEVO moderate and RIVC + DEVO extreme modes were noticeably better than the other methods during the get-warm period of the catalytic converter. This could be primarily attributed to the higher exhaust temperature and higher exhaust flow rates compared to the nominal and RIVC extreme modes. The DEVO moderate and RIVC + DEVO extreme modes had the same fuel consumption penalty (10%) but different exhaust temperatures (220 °C and 250 °C, respectively). Considering the results in Figure 4, DEVO needed to be used moderately to obtain a comparable fuel penalty to the RIVC + DEVO combined mode. The DEVO moderate mode was more effective than the RIVC + DEVO extreme mode in the temperature range [−50, 50 °C] as the exhaust flow rate played a more dominant role in EAT warmup at cold temperatures. However, once the  $T_{EAT\ catalyst\ bed}$  exceeded 50 °C, the combined mode surpassed the DEVO moderate mode, and a heat transfer improvement of up to 103% was achieved for a similar fuel consumption penalty (10%). It can be deduced that the RIVC + DEVO combined mode was the fastest method in heating the EAT unit above 250 °C. It was also more advantageous during the EAT stay-warm period. The low exhaust flow rate led to improved negative heat transfer rates; thus, the EAT unit was maintained longer in the stay-hot period compared to the DEVO moderate and nominal modes. It can

be predicted that an additional mode—a DEVO extreme mode with  $T_{exhaust}$  maintained at 250 °C—would be even more advantageous than the RIVC + DEVO extreme or DEVO moderate modes (Figure 15). This is because it had the highest exhaust temperature and highest exhaust mass flow rate among all cases of interest. However, the fuel consumption penalty up to 20% in this additional mode was extremely high and, thus, not feasible. Therefore, it could not be considered as an option for fast EAT warmup (Figure 15).

#### 4. Conclusions

This study analyzed the potential of different VVT methods (separate or combined) on EAT thermal management through the use of a 1D engine simulation program. At first, the VVT techniques of RIVC and DEVO were applied separately in the model to improve the EAT warmup through increased  $T_{exhaust}$ . Then, the two techniques were combined for further improvement of the  $T_{exhaust}$  and, thus, thermal management of the EAT unit.

The RIVC alone mode was found to be fuel-saving (up to 3%), similar to previous RIVC-related studies. Although RIVC caused a major increase in  $T_{exhaust}$  (up to 55 °C), it was not that effective in the get-warm period of the EAT unit due to the extremely reduced exhaust flow rates (over 30%). However, it was the most advantageous method for the EAT stay-warm period due to the highly improved negative heat transfer rates.

The DEVO alone mode was found to be effective in increasing  $T_{exhaust}$  above 250 °C. However, it not only needed a noticeable reduction in BTE (up to 5%), but also an extreme delay of EVO timing. Both these drawbacks are impractical at low loads for emission minimization. In particular, the high inefficiency due to the aggressive use of DEVO would likely result in increased NO<sub>x</sub>, CO, and PM rates when heating the EAT beyond 250 °C, which is unacceptable.

The RIVC + DEVO combined mode enabled an improvement in BTE (up to 2.5%) compared to the DEVO alone mode while still providing an adequate temperature increase (as high as 55 °C) and maintaining exhaust temperature above 250 °C. This method led to the best improvement in the tradeoff between the BSFC and EAT warmup among all methods through the greatest enhancement of heat transfer rates up to 103%. This led to the EAT system being heated to a higher temperature, in a faster and improved fuel-saving manner, in comparison to the DEVO alone technique. In particular, the lower fuel consumption would be beneficial in maintaining NO<sub>x</sub>, CO, and PM rates at low levels until the EAT is heated beyond 250 °C, which would be more feasible to implement in an automotive engine system compared to the DEVO alone method.

The proposed strategy still imposed a fuel consumption penalty and negatively affected the NO<sub>x</sub> and CO rates when heating the EAT beyond 250 °C. Therefore, the simultaneous use of VVT and EGR (either external or internal) can be explored in the future for improving EAT warmup with reduced NO<sub>x</sub> and CO rates. Another useful study topic for the future would be to combine CDA—a proven fuel-efficient exhaust thermal management technique—with VVT technology in order to further improve EAT warmup in diesel vehicles. VVT can also be combined with engine-independent methods such as afterburners or electrical heating to further enhance EAT warmup in diesel engine systems.

**Funding:** This research received no external funding.

**Data Availability Statement:** All the data are provided within the manuscript.

**Acknowledgments:** The author would like to thank the Lotus Engine Simulation Company for access to the Lotus Engine Simulation Software version 6.01A in this study.

**Conflicts of Interest:** The authors declare no conflict of interest.

## Nomenclature

$\dot{m}$	Mass flow rate, kg/h
$P_e$	Brake power, kW
$T_{exhaust}$	Exhaust temperature, °C
$T_{EAT\ catalyst\ bed}$	EAT catalyst bed temperature, °C
$V_d$	Cylinder displacement, m <sup>3</sup>
$\eta$	Efficiency, %
$\theta$	Burn angle, °
$\theta_b$	Total burn angle, °
AFR	Air-to-fuel ratio
ABDC	After bottom dead center
ATDC	After top dead center
BBDC	Before bottom dead center
BTDC	Before top dead center
<i>BMEP</i>	Brake mean effective pressure, bar
<i>BSFC</i>	Brake specific fuel consumption, g/kWh
BDC	Bottom dead center
CA	Crank angle, °
CDA	Cylinder deactivation
CR	Compression ratio
DEVO	Delayed exhaust valve opening, °
DFI	Delayed fuel injection, °
EAT	Exhaust after-treatment
EVC	Exhaust valve closure, °
EVO	Exhaust valve opening, °
FIR	Fuel injection rate, mm <sup>3</sup> /injection
<i>FMEP</i>	Friction mean effective pressure, bar
IMEP	Indicated mean effective pressure, bar
IVC	Intake valve closure, °
IVO	Intake valve opening, °
LES	Lotus engine simulation
NO <sub>x</sub>	Nitrogen oxide
<i>PMEP</i>	Pumping mean effective pressure, bar
RIVC	Retarded intake valve closure, °
RPM	Revolutions per minute
TDC	Top dead center
TWC	Three-way catalytic convertor
VVT	Variable valve timing

## References

1. Dieselnet. Emission Standards, European Union, Passenger Cars. Available online: <https://www.dieselnet.com/standards/eu/ld.php#stds> (accessed on 23 April 2023).
2. Dieselnet. Emission Standards, United States, Marine Diesel Engines. Available online: <https://www.dieselnet.com/standards/us/marine.php#stds> (accessed on 23 April 2023).
3. Rahman, S.A.; Rizwanul Fattah, I.M.; Ong, H.C.; Zamri, M.F.M.A. State-of-the-Art of Strategies to Reduce Exhaust Emissions from Diesel Engine Vehicles. *Energies* **2021**, *14*, 1766. [CrossRef]
4. Zhao, J.; Wei, Q.; Wang, S.; Ren, X. Progress of ship exhaust gas control technology. *Energies* **2021**, *799*, 149437. [CrossRef]
5. Tang, X.; Wang, P.; Zhang, Z.; Zhang, F.; Shi, L.; Deng, K. Effects of high-pressure and donor-cylinder exhaust gas recirculation on fuel economy and emissions of marine diesel engines. *Fuel* **2022**, *309*, 122226. [CrossRef]
6. Rakopoulos, C.D.; Rakopoulos, D.C.; Mavropoulos, G.C.; Kosmadakis, G.M. Investigating the EGR rate and temperature impact on diesel engine combustion and emissions under various injection timings and loads by comprehensive two-zone modeling. *Energy* **2018**, *157*, 990–1014. [CrossRef]
7. Chauhan, B.V.; Sayyed, I.; Vedrantam, A.; Garg, A.; Bharti, S.; Shukla, M. State of the Art in Low-Temperature Combustion Technologies: HCCI, PCCI, and RCCI. In *Advanced Combustion for Sustainable Transport*; Springer: Singapore, 2022; pp. 95–139.
8. Mansor, M.R.A.; Abbood, M.M.; Mohamad, T.I. The influence of varying hydrogen-methane-diesel mixture ratio on the combustion characteristics and emission of a direct injection diesel engine. *Fuel* **2017**, *190*, 281–291. [CrossRef]

9. Hasan, A.O.; Osman, A.I.; Al-Muhtaseb, A.H.; Al-Rawashdeh, H.; Abu-Jrai, A.; Ahmad, R.; Gomaa, M.R.; Deka, T.J.; Rooney, D.W. An experimental study of engine characteristics and tailpipe emissions from modern DI diesel engine fuelled with methanol/diesel blends. *Fuel Process. Technol.* **2021**, *220*, 106901. [[CrossRef](#)]
10. Freitas, E.S.D.C.; Guarieiro, L.L.N.; da Silva, M.V.I.; Amparo, K.K.D.S.; Machado, B.A.S.; Guerreiro, E.T.d.A.; de Jesus, J.F.C.; Torres, E.A. Emission and Performance Evaluation of a Diesel Engine Using Addition of Ethanol to Diesel/Biodiesel Fuel Blend. *Energies* **2022**, *15*, 2988. [[CrossRef](#)]
11. Votsmeier, M.; Kreuzer, T.; Gieshoff, J.; Lepperhoff, G. Automobile exhaust control. *Ullmann's Encycl. Ind. Chem.* **2009**, *4*, 407–424.
12. Konstandopoulos, A.G.; Kostoglou, M.; Beatrice, C.; Di Blasio, G.; Imren, A.; Denbratt, I. Impact of combination of EGR, SCR, and DPF technologies for the low-emission rail diesel engines. *Emiss. Control Sci. Technol.* **2015**, *1*, 213–225. [[CrossRef](#)]
13. Gerald Liu, Z.; Munnannur, A. Future Diesel Engines. In *Design and Development of Heavy Duty Diesel Engines: A Handbook*; Springer: Singapore, 2020; pp. 887–914.
14. Kašpar, J.; Fornasiero, P.; Hickey, N. Automotive catalytic converters: Current status and some perspectives. *Catal. Today* **2003**, *77*, 419–449. [[CrossRef](#)]
15. Girard, J.; Cavataio, G.; Snow, R.; Lambert, C. Combined Fe-Cu SCR systems with optimized ammonia to NOx ratio for diesel NOx control. *SAE Int. J. Fuels Lubr.* **2009**, *1*, 603–610. [[CrossRef](#)]
16. Song, X.; Surenahalli, H.; Naber, J.; Parker, G.; Johnson, J.H. *Experimental and Modeling Study of a Diesel Oxidation Catalyst (DOC) Under Transient and CPF Active Regeneration Conditions*; SAE Technical Paper, No. 2013-01-1046; SAE International: Warrendale, PA, USA, 2013.
17. Hou, X.; Ma, Y.; Peng, F.; Yan, F.; Zhang, X. Research on temperature characteristics of dpf regeneration technology based on catalytic combustion of fuel injection. In Proceedings of the 2010 Asia-Pacific power and energy engineering conference (APPEEC), Chengdu, China, 28–31 March 2010; IEEE: Manhattan, NY, USA, 2010; pp. 1–4.
18. Charlton, S.; Dollmeyer, T.; Grana, T. Meeting the US heavy-duty EPA 2010 standards and providing increased value for the customer. *SAE Int. J. Commer. Veh.* **2010**, *3*, 101–110. [[CrossRef](#)]
19. Feng, R.; Hu, X.; Li, G.; Sun, Z.; Ye, M.; Deng, B. Exploration on the emissions and catalytic reactors interactions of a non-road diesel engine through experiment and system level simulation. *Fuel* **2023**, *342*, 127746. [[CrossRef](#)]
20. Honardar, S.; Busch, H.; Schnorbus, T.; Severin, C.; Kolbeck, A.F.; Korfer, T. *Exhaust Temperature Management for Diesel Engines Assessment of Engine Concepts and Calibration Strategies with Regard to Fuel Penalty*; SAE Technical Paper, No. 2011-24-0176; SAE International: Warrendale, PA, USA, 2011.
21. Munnannur, A.; Ottinger, N.; Gerald Liu, Z. Thermal Management of Exhaust Aftertreatment for Diesel Engines. In *Handbook of Thermal Management of Engines*; Springer: Singapore, 2022; pp. 29–90.
22. Hu, J.; Wu, Y.; Yu, Q.; Liao, J.; Cai, Z. Heating and storage: A review on exhaust thermal management applications for a better trade-off between environment and economy in ICEs. *Appl. Therm. Eng.* **2023**, *220*, 119782. [[CrossRef](#)]
23. Wang, J.; Wang, B.; Cao, Z. Experimental research on exhaust thermal management control strategy for diesel particulate filter active regeneration. *Int. J. Automot. Technol.* **2020**, *21*, 1185–1194. [[CrossRef](#)]
24. Stadlbauer, S.; Waschl, H.; Schilling, A.; del Re, L. *DOC Temperature Control for Low Temperature Operating Ranges with Post and Main Injection Actuation*; SAE Technical Paper, No. 2013-01-1580; SAE International: Warrendale, PA, USA, 2013.
25. Wang, Z.; Shen, L.; Lei, J.; Yao, G.; Wang, G. Impact characteristics of post injection on exhaust temperature and hydrocarbon emissions of a diesel engine. *Energy Rep.* **2022**, *8*, 4332–4343. [[CrossRef](#)]
26. Nie, X.; Bi, Y.; Liu, S.; Shen, L.; Wan, M. Impacts of different exhaust thermal management methods on diesel engine and SCR performance at different altitude levels. *Fuel* **2022**, *324*, 124747. [[CrossRef](#)]
27. Anbarasu, M.; Ramani, V.S. *Improvement of SCR Thermal Management System and Emissions Reduction through Combustion Optimization*; SAE Technical Paper, No. 2022-28-0482; SAE International: Warrendale, PA, USA, 2022.
28. Hamedi, M.R.; Doustdar, O.; Tsolakis, A.; Hartland, J. Thermal energy storage system for efficient diesel exhaust aftertreatment at low temperatures. *Appl. Energy* **2019**, *235*, 874–887. [[CrossRef](#)]
29. Hamedi, M.R.; Doustdar, O.; Tsolakis, A.; Hartland, J. Energy-efficient heating strategies of diesel oxidation catalyst for low emissions vehicles. *Energy* **2021**, *230*, 120819. [[CrossRef](#)]
30. Clenci, A.; Berquez, J.; Stoica, R.; Niculescu, R.; Cioc, B.; Zaharia, C.; Iorga-Simán, V. Experimental investigation of the effect of an afterburner on the light-off performance of an exhaust after-treatment system. *Energy Rep.* **2022**, *8*, 406–418.
31. Dinler, N.; Aktas, F.; Taskin, S.; Karaaslan, S.; Yucel, N. Effects of Preheater Load and Location on the Catalytic Converter Efficiency during Cold Start and Idling Conditions. *Isi Bilimi Tekniği Dergisi* **2021**, *41*, 239–247. [[CrossRef](#)]
32. Brück, R.; Presti, M.; Keck, M.; Dengler, J.; Faiß, M. Thermal management on demand; the exhaust aftertreatment solution for future heavy duty application. In *Internationaler Motorenkongress 2021*; Springer Vieweg: Wiesbaden, Germany, 2021; pp. 387–399.
33. Gehrke, S.; Kovács, D.; Eilts, P.; Rempel, A.; Eckert, P. Investigation of VVA-based exhaust management strategies by means of a HD single cylinder research engine and rapid prototyping systems. *SAE Int. J. Commer. Veh.* **2013**, *6*, 47–61. [[CrossRef](#)]
34. Gosala, D.B.; Ramesh, A.K.; Allen, C.M.; Joshi, M.C.; Taylor, A.H.; Van Voorhis, M.; Shaver, G.M.; Farrell, L.; Koeberlein, E.; McCarthy, J., Jr.; et al. Diesel engine aftertreatment warm-up through early exhaust valve opening and internal exhaust gas recirculation during idle operation. *Int. J. Eng. Res.* **2018**, *19*, 758–773. [[CrossRef](#)]

35. Roberts, L.; Magee, M.; Shaver, G.; Garg, A.; McCarthy, J.; Koeberlein, E.; Holloway, E.; Shute, R.; Koeberlein, D.; Nielsen, D. Modeling the impact of early exhaust valve opening on exhaust after-treatment thermal management and efficiency for compression ignition engines. *Int. J. Eng. Res.* **2015**, *16*, 773–794. [CrossRef]
36. Basaran, H.U.; Ozsoysal, O.A. Effects of application of variable valve timing on the exhaust gas temperature improvement in a low-loaded diesel engine. *Appl. Therm. Eng.* **2017**, *122*, 758–767. [CrossRef]
37. Morris, A.; McCarthy, J. *The Effect of Heavy-Duty Diesel Cylinder Deactivation on Exhaust Temperature, Fuel Consumption, and Turbocharger Performance Up to 3 Bar BMEP*; SAE Technical Paper, No. 2020-01-1407; SAE International: Warrendale, PA, USA, 2020.
38. Ramesh, A.K.; Gosala, D.B.; Allen, C.; Joshi, M.; McCarthy, J., Jr.; Farrell, L.; Koeberlein, E.D.; Shaver, G.M. *Cylinder Deactivation for Increased Engine Efficiency and Aftertreatment Thermal Management in Diesel Engines*; SAE Technical Paper, 2018-01-0384; SAE International: Warrendale, PA, USA, 2018.
39. Basaran, H.U. Fuel-saving Exhaust after-treatment Management on a Sparkignition Engine System via Cylinder Deactivation Method. *Isı Bilimi ve Tekniği Dergisi* **2018**, *38*, 87–98.
40. Ramesh, A.K.; Shaver, G.M.; Allen, C.M.; Nayyar, S.; Gosala, D.B.; Caicedo Parra, D.; Koeberlein, E.; McCarthy, J., Jr.; Nielsen, D. Utilizing low airflow strategies, including cylinder deactivation, to improve fuel efficiency and aftertreatment thermal management. *Int. J. Eng. Res.* **2017**, *18*, 1005–1016. [CrossRef]
41. Garcia, E.; Triantopoulos, V.; Trzaska, J.; Taylor, M.; Li, J.; Boehman, A.L. Extreme Miller cycle with high intake boost for improved efficiency and emissions in heavy-duty diesel engines. *Int. J. Eng. Res.* **2023**, *24*, 552–566. [CrossRef]
42. Liu, F.; Liu, B.; Zhang, J.; Wan, P.; Li, B. Study on a Novel Variable Valve Timing and Lift Mechanism for a Miller Cycle Diesel Engine. *Energies* **2022**, *15*, 8521. [CrossRef]
43. Gao, J.; Tian, G.; Sornioti, A.; Karci, A.E.; Di Palo, R. Review of thermal management of catalytic converters to decrease engine emissions during cold start and warm up. *Appl. Therm. Eng.* **2019**, *147*, 177–187. [CrossRef]
44. Basaran, H.U. Effects of Intake Valve Lift Form Modulation on Exhaust Temperature and Fuel Economy of a Low-loaded Automotive Diesel Engine. *Int. J. Automot. Sci. Technol.* **2021**, *5*, 85–98. [CrossRef]
45. Bharath, A.N.; Kalva, N.; Reitz, R.D.; Rutland, C.J. Use of early exhaust valve opening to improve combustion efficiency and catalyst effectiveness in a multi-cylinder RCCI engine system: A simulation study. In Proceedings of the ASME 2014 Internal Combustion Engine Division Fall Technical Conference, Volume 1: Large Bore Engines; Fuels; Advanced Combustion; Emissions Control Systems, Columbus, IN, USA, 19–22 October 2014; American Society of Mechanical Engineers: New York, NY, USA, 2014; V001T03A011.
46. Tan, P.; Duan, L.; Li, E.; Hu, Z.; Lou, D. *Experimental Study on Thermal Management Strategy of the Exhaust Gas of a Heavy-Duty Diesel Engine Based on In-Cylinder Injection*; SAE Technical Paper, No. 2020-01-0621; SAE International: Warrendale, PA, USA, 2020.
47. Garg, A.; Magee, M.; Ding, C.; Roberts, L.; Shaver, G.; Koeberlein, E.; Shute, R.; Koeberlein, D.; McCarthy, J.J.; Nielsen, D. Fuel-efficient exhaust thermal management using cylinder throttling via intake valve closing timing modulation. *Proc. Inst. Mech. Eng. Part D J. Automob. Eng.* **2016**, *230*, 470–478. [CrossRef]
48. Basaran, H.U. Utilizing exhaust valve opening modulation for fast warm-up of exhaust after-treatment systems on highway diesel vehicles. *Int. J. Automot. Sci. Technol.* **2020**, *4*, 10–22. [CrossRef]
49. He, X.; Durrett, R.P.; Sun, Z. Late intake valve closing as an emissions control strategy at Tier 2 Bin 5 engine-out NOx level. *SAE Int. J. Eng.* **2009**, *1*, 427–443. [CrossRef]
50. Joshi, M.C.; Gosala, D.; Shaver, G.M.; McCarthy, J.; Farrell, L. Exhaust valve profile modulation for improved diesel engine curb idle aftertreatment thermal management. *Int. J. Eng. Res.* **2021**, *22*, 3179–3195. [CrossRef]
51. Schwoerer, J.A.; Kumar, K.; Ruggiero, B.; Swanbon, B. *Lost-Motion VVA Systems for Enabling Next Generation Diesel Engine Efficiency and after-Treatment Optimization*; SAE Technical Paper, No. 2010-01-1189; SAE International: Warrendale, PA, USA, 2010.
52. Piano, A.; Millo, F.; Di Nunno, D.; Gallone, A. *Numerical Analysis on the Potential of Different Variable Valve Actuation on a Light-Duty Diesel Engine for Improving Exhaust System Warm Up*; SAE Technical Paper, No. 2017-24-0024; SAE International: Warrendale, PA, USA, 2017.
53. Joshi, M.C.; Gosala, D.B.; Allen, C.M.; Vos, K.; Voorhis, M.V.; Taylor, A.; Shaver, G.M.; McCarthy, J.J.; Stretch, D.; Koeberlein, E.; et al. Reducing diesel engine drive cycle fuel consumption through use of cylinder deactivation to maintain aftertreatment component temperature during idle and low load operating conditions. *Front. Mech. Eng.* **2017**, *3*, 8. [CrossRef]
54. Allen, C.M.; Joshi, M.C.; Gosala, D.B.; Shaver, G.M.; Farrell, L.; McCarthy, J. Experimental assessment of diesel engine cylinder deactivation performance during low-load transient operations. *Int. J. Eng. Res.* **2021**, *22*, 606–615. [CrossRef]
55. Serrano, J.R.; Arnau, F.J.; Martin, J.; Aunon, A. Development of a variable valve actuation control to improve diesel oxidation catalyst efficiency and emissions in a light duty diesel engine. *Energies* **2020**, *13*, 4561. [CrossRef]
56. Lotus Engineering Software. *Lotus Engine Simulation (LES) Version 6.01A*; Lotus Engineering: Norfolk, UK.
57. Lotus Engineering. Getting Started with Lotus Engine Simulation. Available online: <https://lotusproactive.files.wordpress.com/2013/08/getting-started-with-lotus-engine-simulation.pdf> (accessed on 23 April 2023).
58. Pearson, R.J.; Bassett, M.D.; Fleming, N.P.; Rodemann, T. *Lotus Engineering Software—An Approach to Model-Based Design*; Lotus Engineering: Norfolk, UK, 2002.
59. Sezer, İ. Alternative gaseous fuels in port fuel injection spark ignition engines. *J. Energy Inst.* **2011**, *84*, 207–214. [CrossRef]



60. Allawi, M.K.; Mejbil, M.K.; Oudah, M.H. Variable valve timing (VVT) modelling by Lotus engine simulation software. *Int. J. Automot. Mech. Eng.* **2020**, *17*, 8397–8410. [[CrossRef](#)]
61. Mishra, R.; Saad, S.M. Simulation based study on improving the transient response quality of turbocharged diesel engines. *J. Qual. Maint. Eng.* **2017**, *23*, 297–309. [[CrossRef](#)]
62. Vos, K.R.; Shaver, G.M.; Joshi, M.C.; McCarthy, J., Jr. Implementing variable valve actuation on a diesel engine at high-speed idle operation for improved aftertreatment warm-up. *Int. J. Eng. Res.* **2020**, *21*, 1134–1146. [[CrossRef](#)]
63. Heywood, J.B. *Internal Combustion Engine Fundamentals*; McGraw-Hill, Inc., Book Company: New York, NY, USA, 1988.
64. Sandoval, D.; Heywood, J.B. *An Improved Friction Model for Spark-Ignition Engines*; SAE Technical Paper No. 2003-01-0725; SAE International: Warrendale, PA, USA, 2003.
65. Stanton, D.W. Systematic development of highly efficient and clean engines to meet future commercial vehicle greenhouse gas regulations. *SAE Int. J. Eng.* **2013**, *6*, 1395–1480. [[CrossRef](#)]
66. Watson, N.; Pilley, A.D.; Marzouk, M. *A Combustion Correlation for Diesel Engine Simulation*; SAE Technical Paper No. 800029; SAE International: Warrendale, PA, USA, 1980.
67. Annand, W.J.D. Heat transfer in the cylinders of reciprocating internal combustion engines. *Proc. Inst. Mech. Eng.* **1963**, *177*, 973–996.
68. Incropera, P.; DeWitt, D.; Bergman, T.; Lavine, A. *Fundamentals of Heat and Mass Transfer*; John Wiley and Sons: Minneapolis, MN, USA, 2007.

**Disclaimer/Publisher’s Note:** The statements, opinions and data contained in all publications are solely those of the individual author(s) and contributor(s) and not of MDPI and/or the editor(s). MDPI and/or the editor(s) disclaim responsibility for any injury to people or property resulting from any ideas, methods, instructions or products referred to in the content.